Deutsche Gesellschaft für Nuklearmedizin e.V.

SUMMER SCHOOL 2016

Translational Research in Molecular Imaging and Radionuclide Therapy

Overview Molecular Imaging

PET and SPECT

UNIKLINIK RWTH AACHEN
KLINIK FÜR NUKLEARMEDIZIN
F.M. Mottaghy

Deutsche Gesellschaft für Nuklearmedizin e.V.
SUMMER SCHOOL 2016

Berlin, August 25 - 27, 2016

Medical imaging and the pathology cascade

Molecular/Cellular disturbance

↓

Alterations in physiology

↓

Structural lesion

Diagnostic approach

Nuclear/Molecular Medicine

Radiology

Molecular interactions of radiolabeled probes

In vivo imaging of biological processes with radiolabeled molecular probes

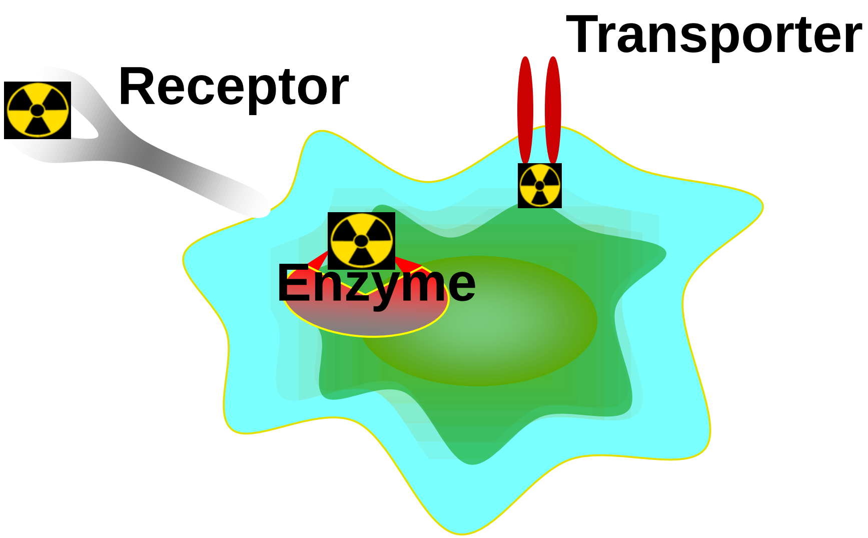

Mechanism of localization

Visualization of overexpression or increased activity of:

- Receptors
- Enzymes
- Transporters

Nuclear Molecular Imaging

In vivo imaging of biological processes with

radiolabeled molecular probes

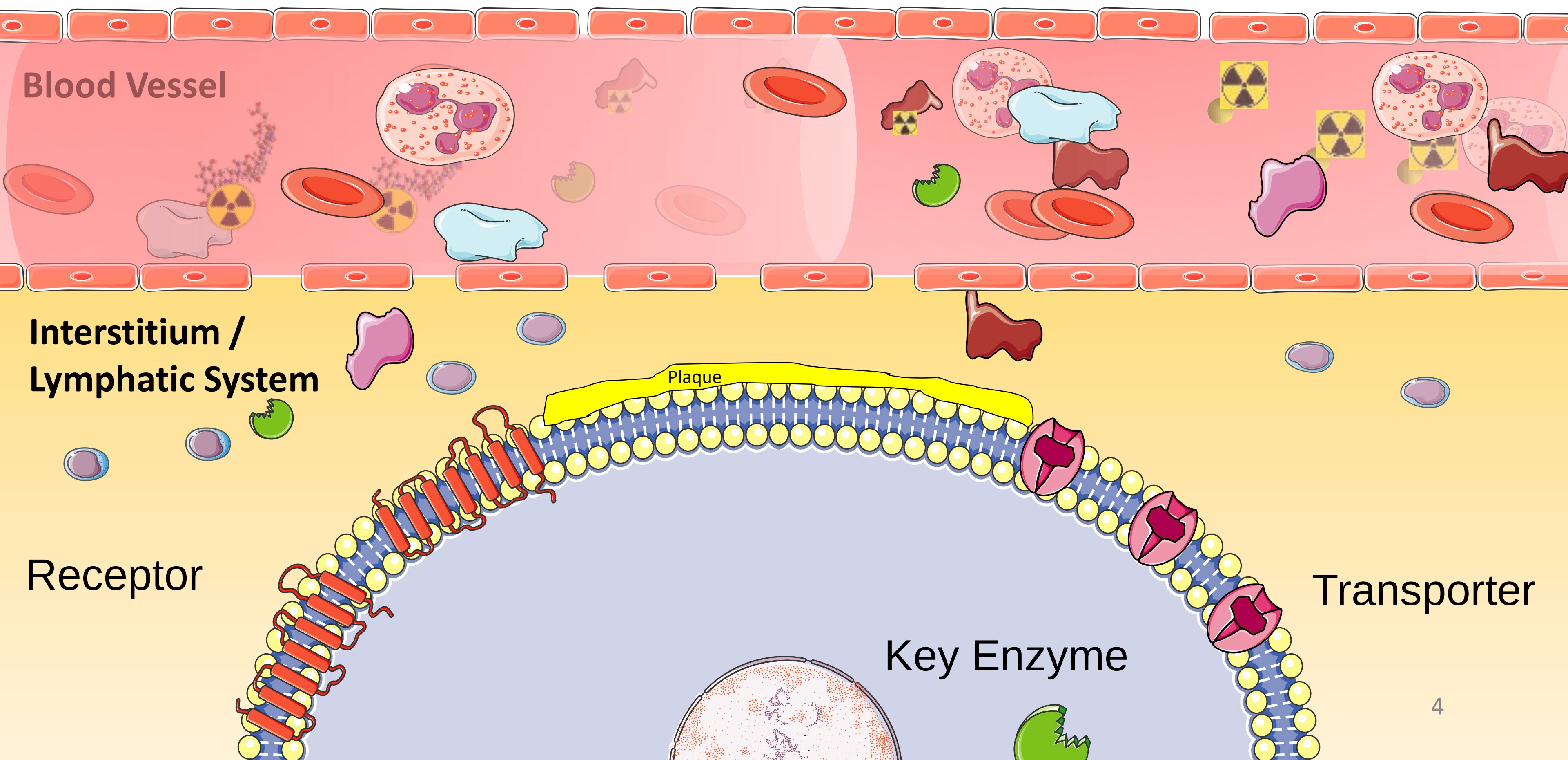

Molecular Probes (Tracers)

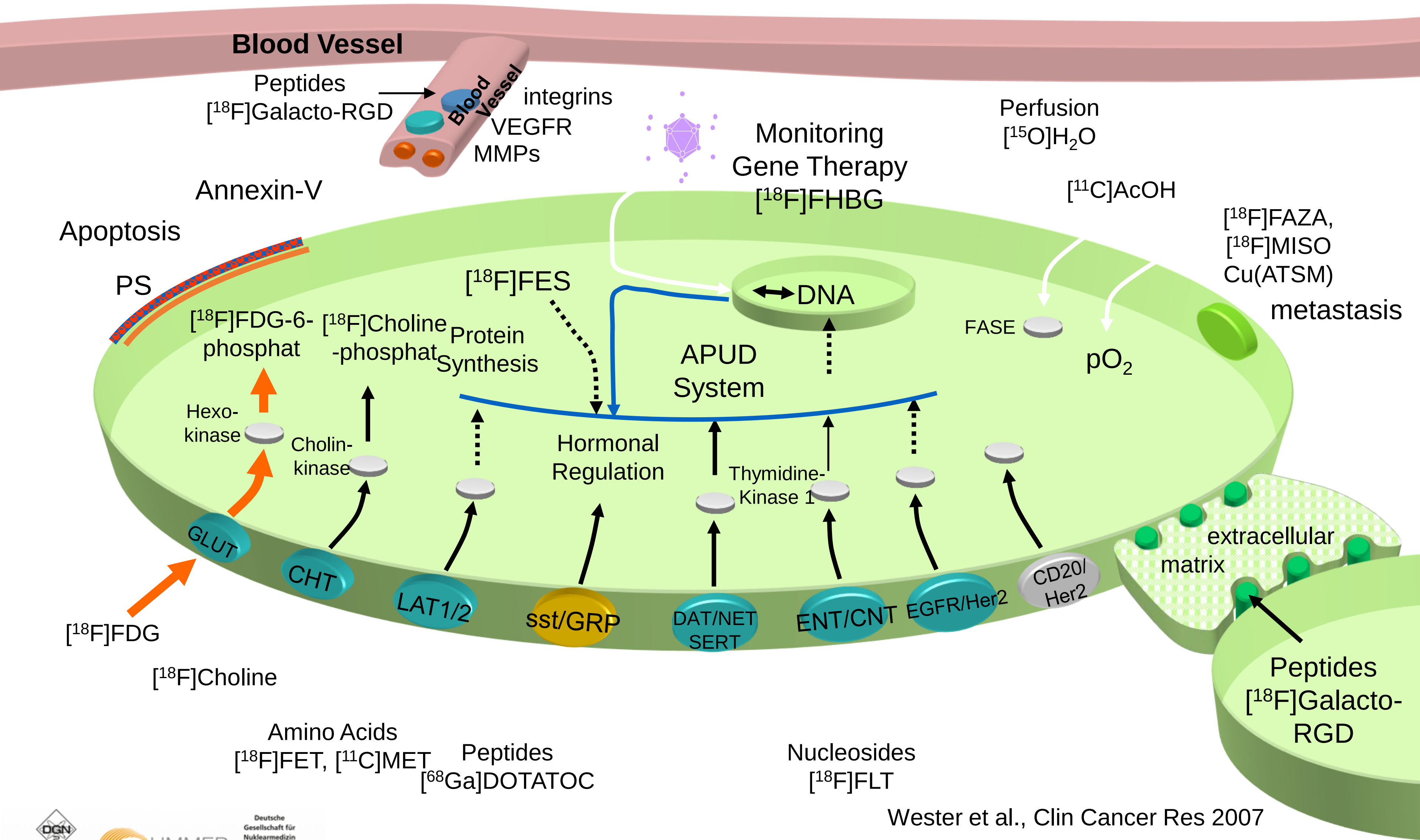

Wester et al., Clin Cancer Res 2007

COMPARTMENT MODEL

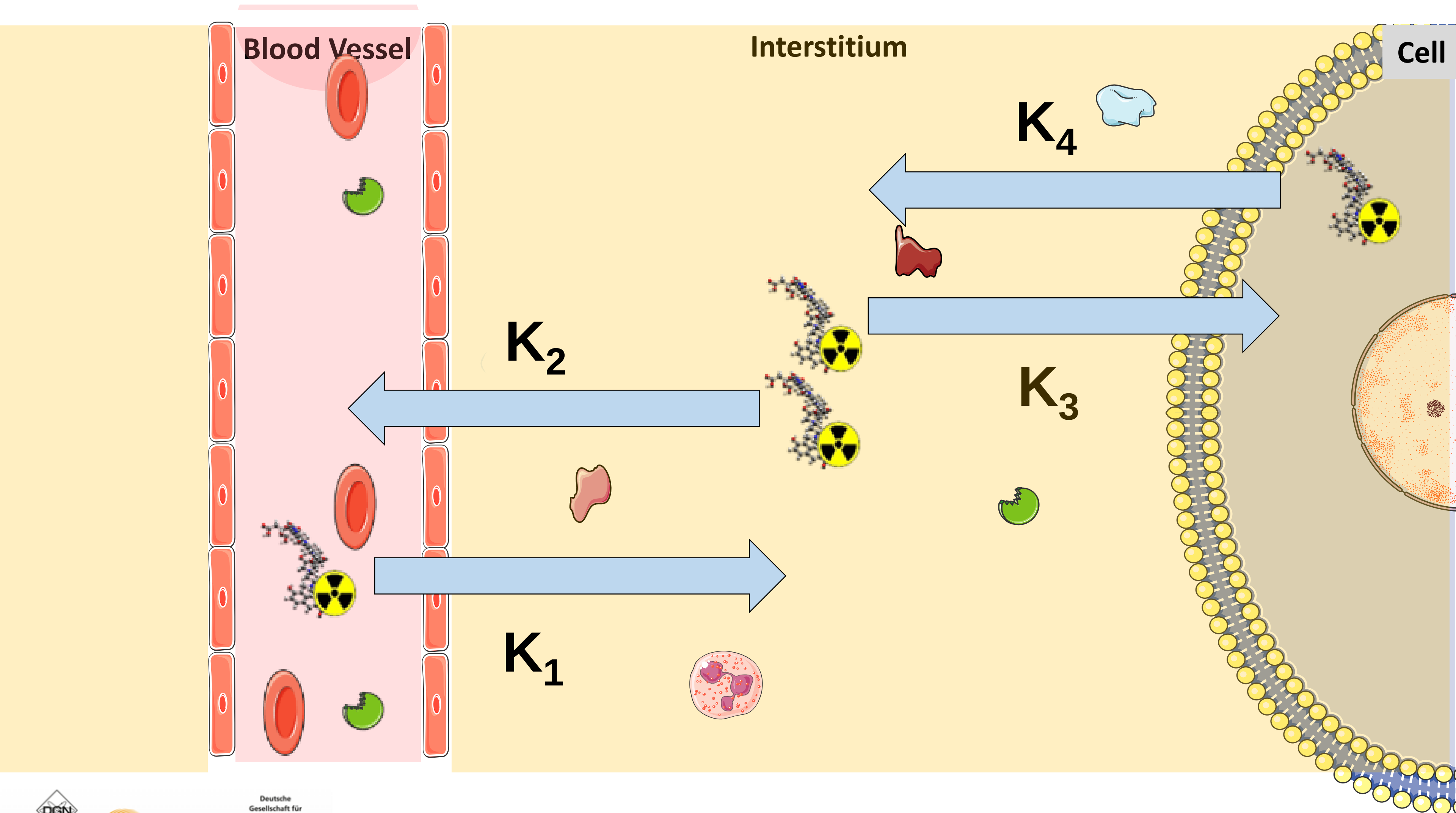

Steps to molecular image acquisition

1. Radionuclide

2. Synthesis of radiopharmaceutical

3. Radiopharmaceutical

4. Application

5. Scan

6. Image

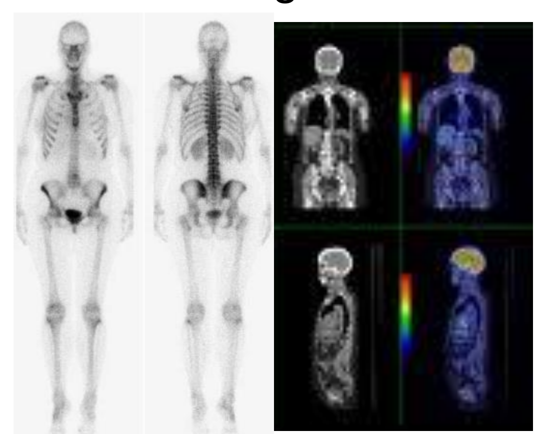

Planar Scintigraphy

^{99m}Tc

6h HWZ
140 keV

Nuklid

target-specific radiopharmaceuticals

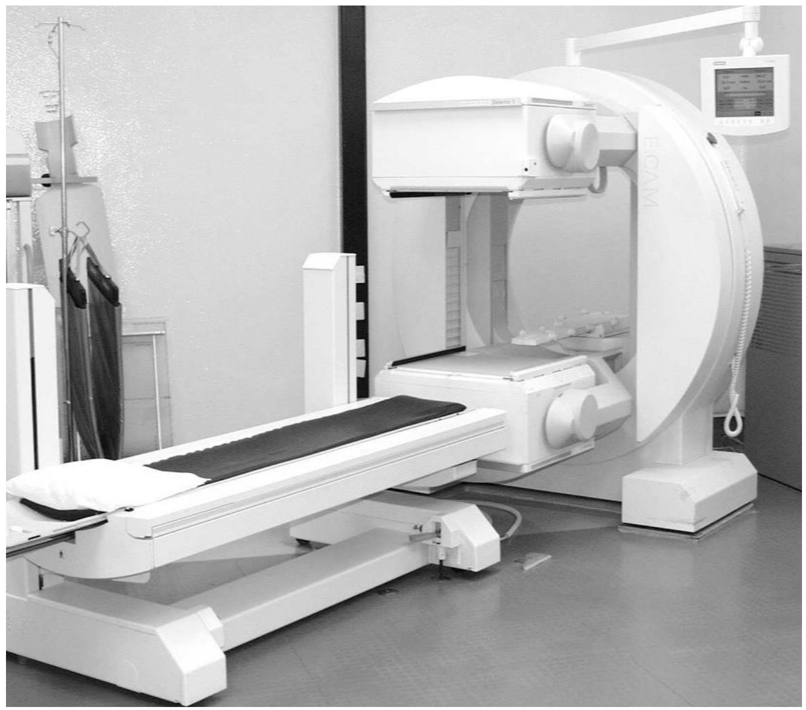

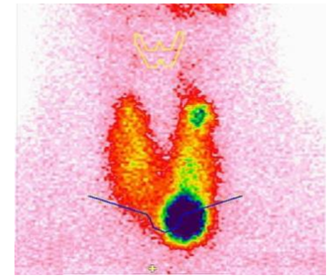

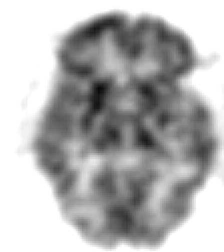

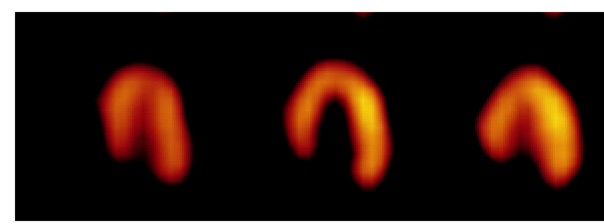

Bone-Scintigraphy (^{99m}Tc-MDP)

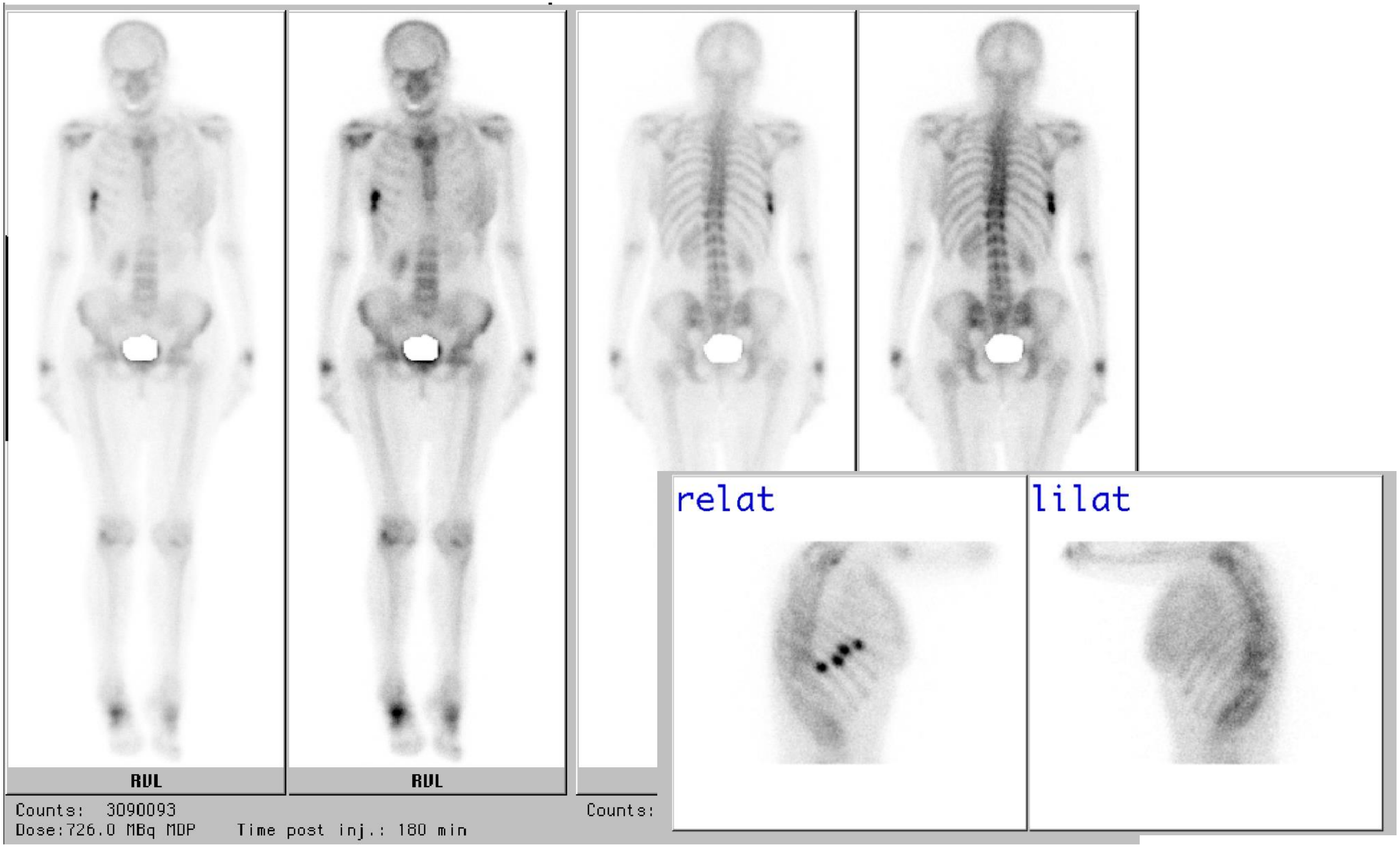

Single Photon Emission Computed Tomography (SPECT)

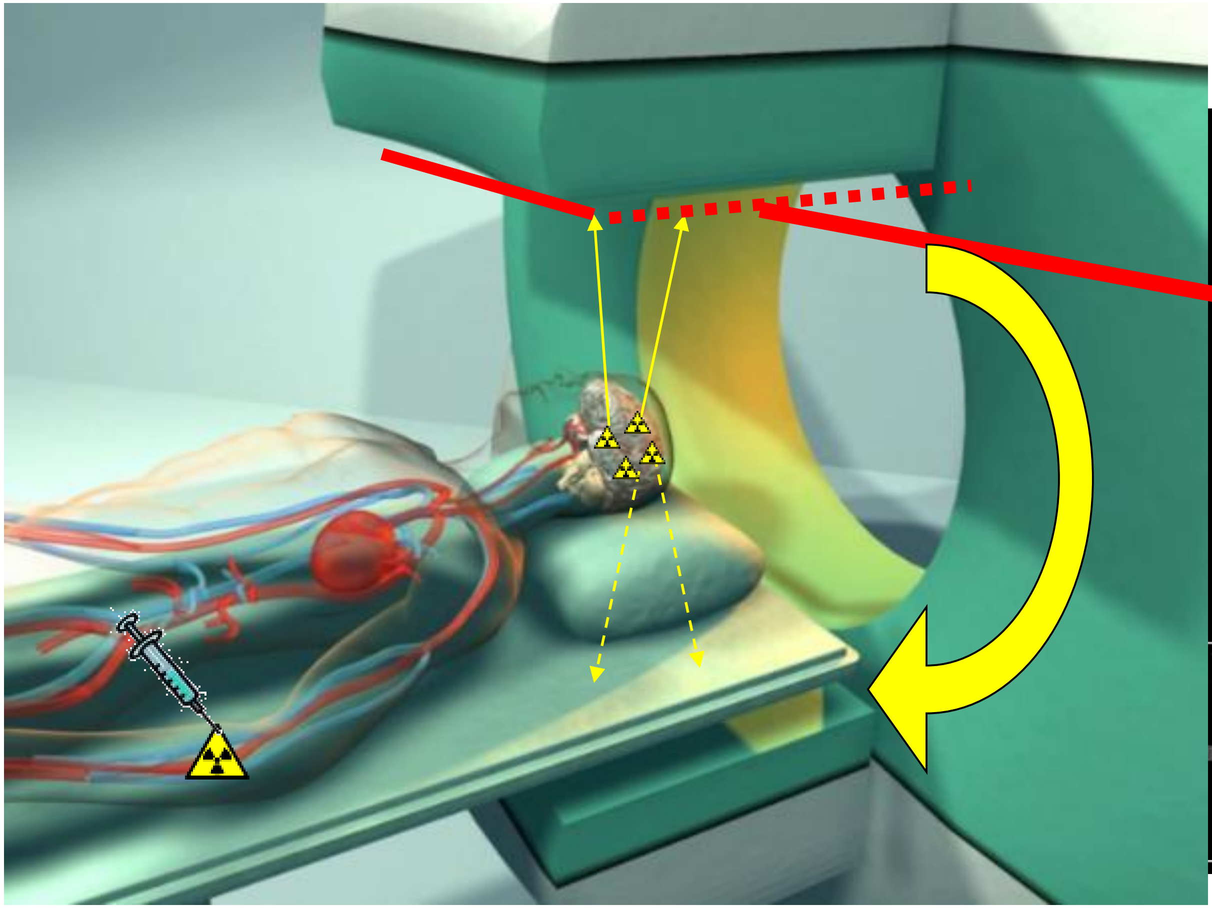

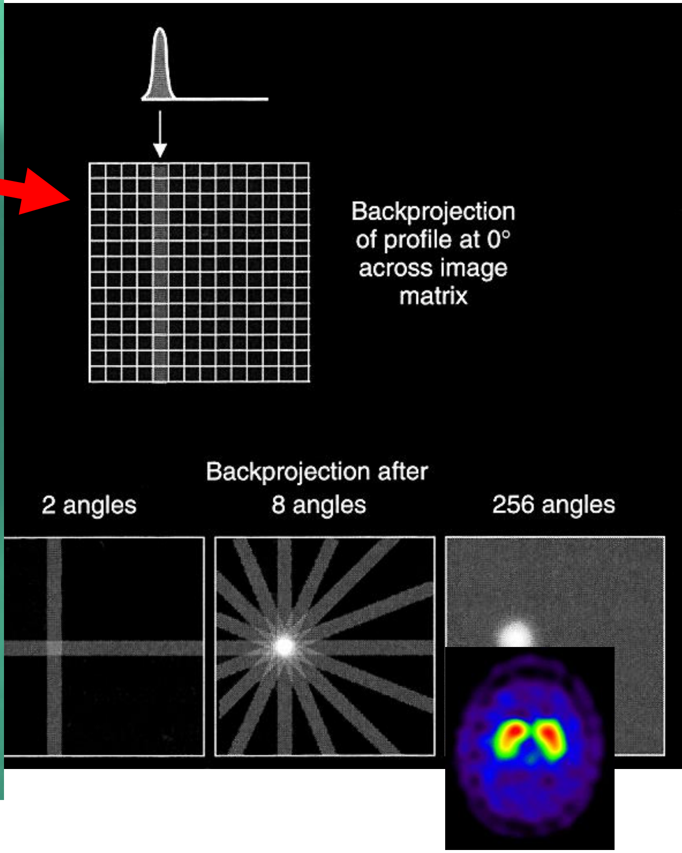

Myocardial SPECT

Cardiovascular disease, ergometry until 75 Watt

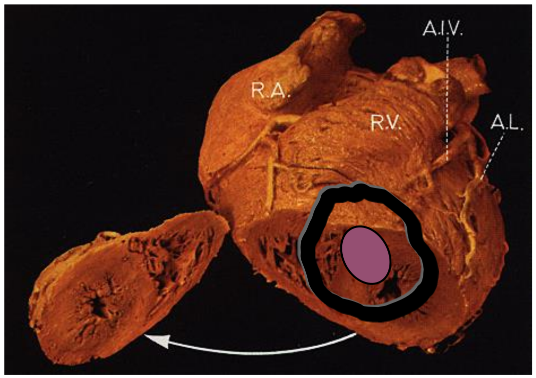

short axis

horiz. long axis

vert. long axis

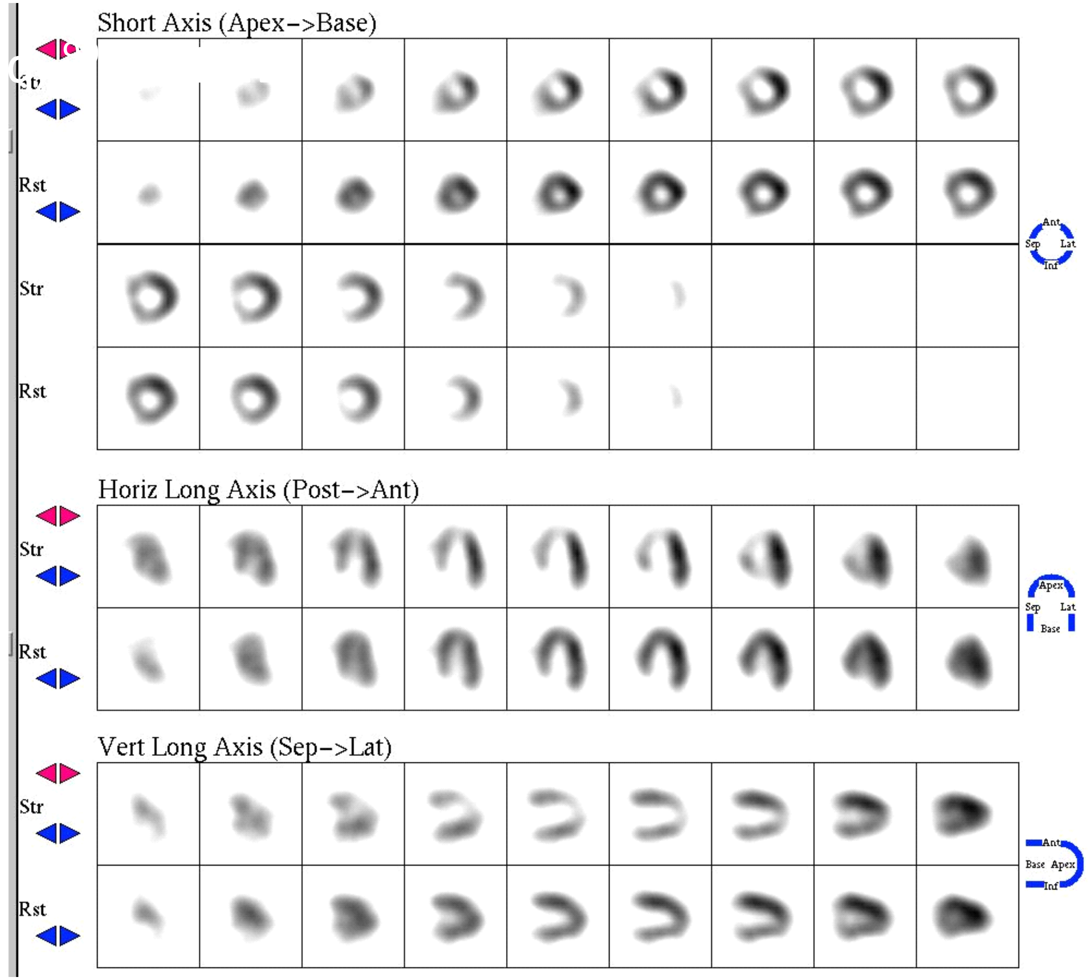

Positronen-Emissions-Tomographie (PET)


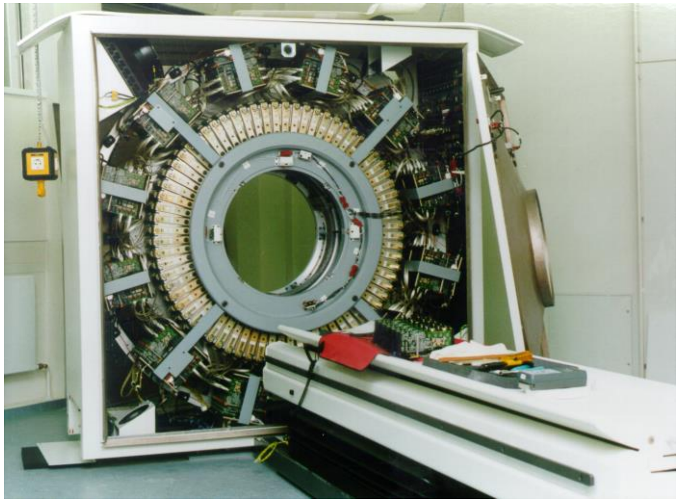


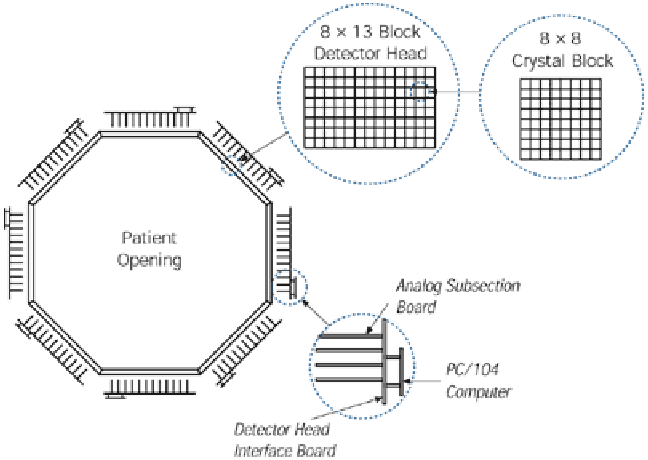

^{18}F-Fluoride PET

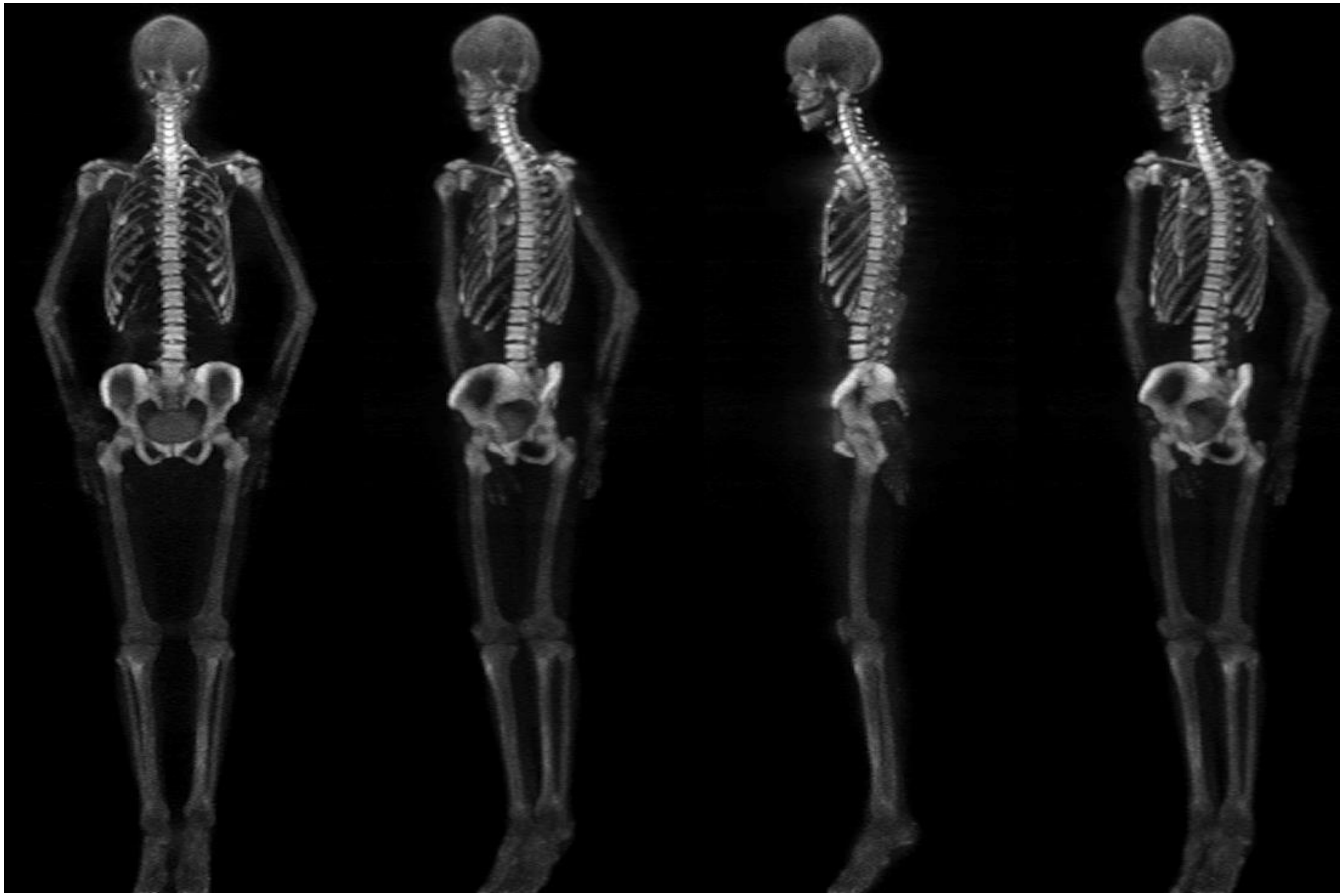

Fluordeoxyglucose-PET (Sarkoidosis)

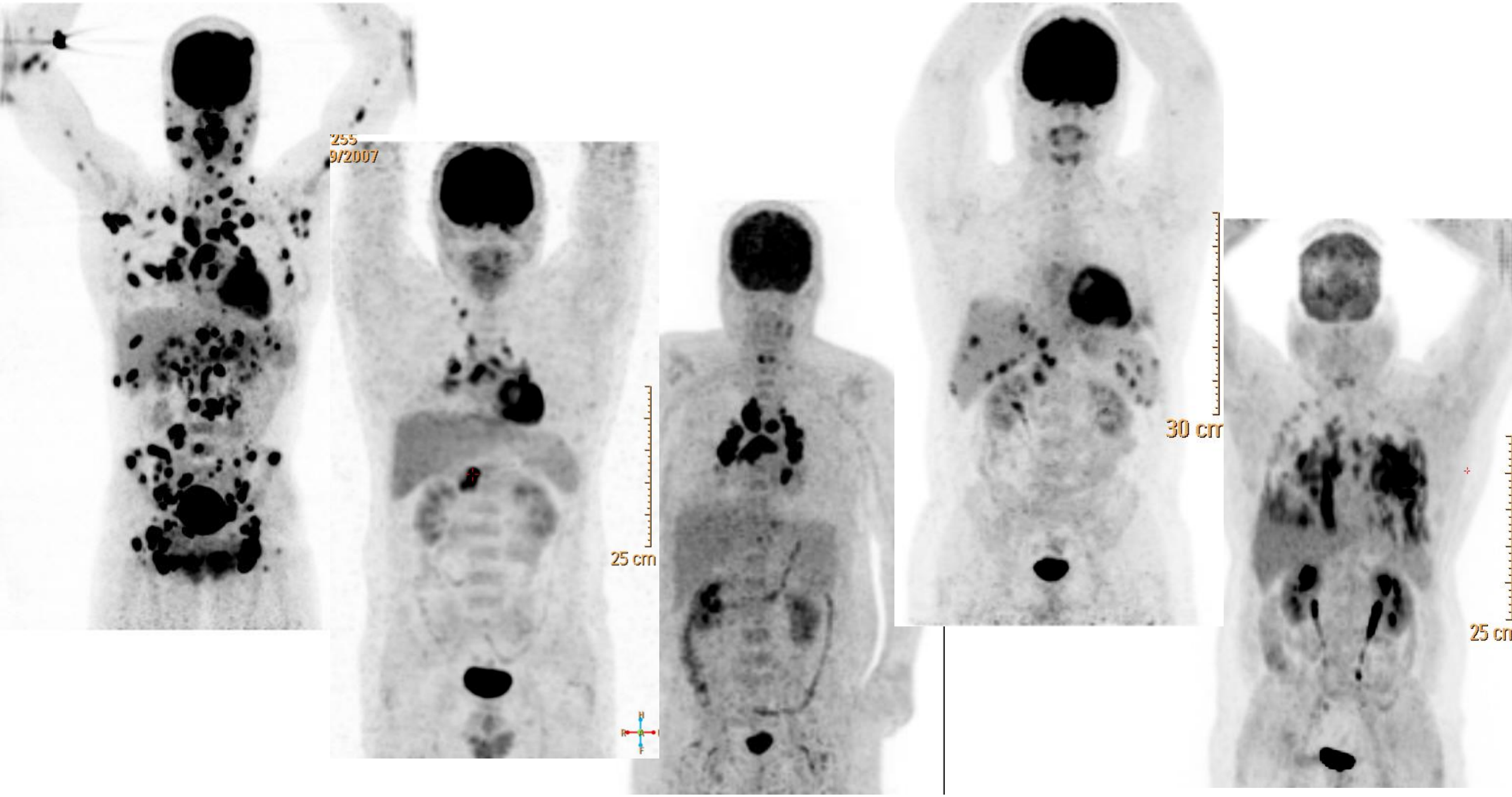

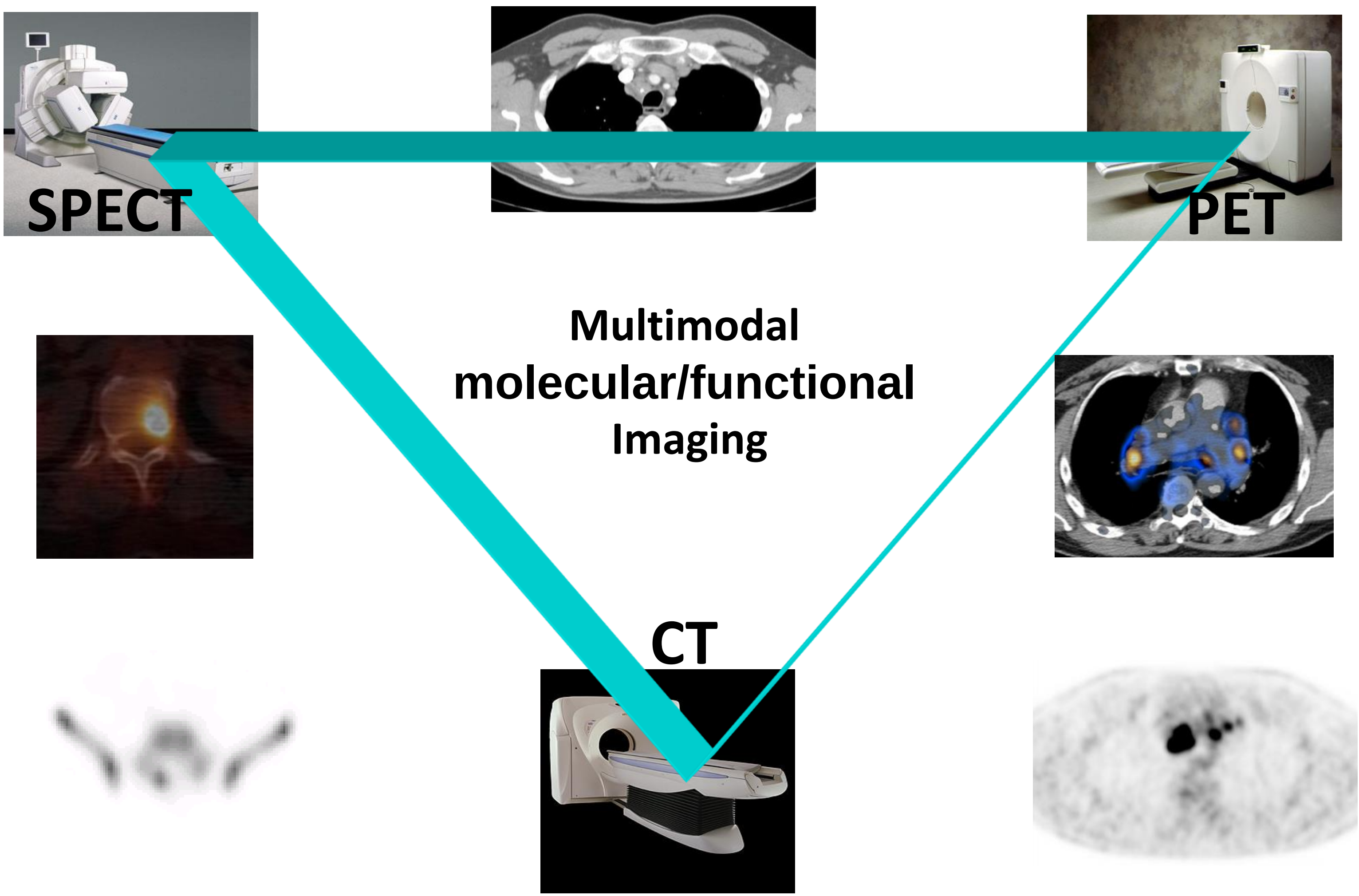
SPECT
PET
Multimodal
molecular/functional
Imaging
CT

SPECT/CT

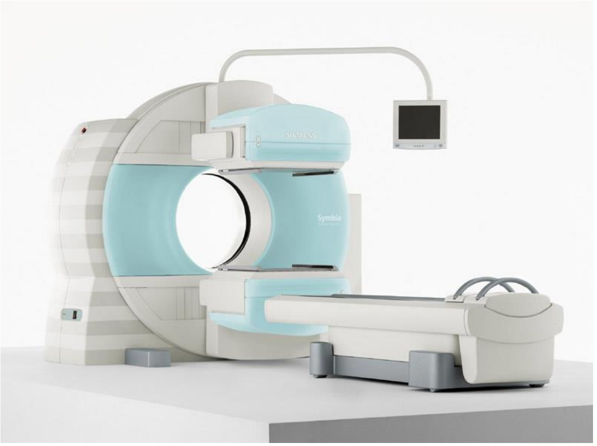

SPECT/CT Prostate Cancer
Bone Scan

- Age 68 yrs., Post OP
- PSA increased
- Bone Scan,
  (745 MBq Tc-99m-HDP)
- SPECT/CT

Staging I

Staging II
Pedicle of vertebral arch

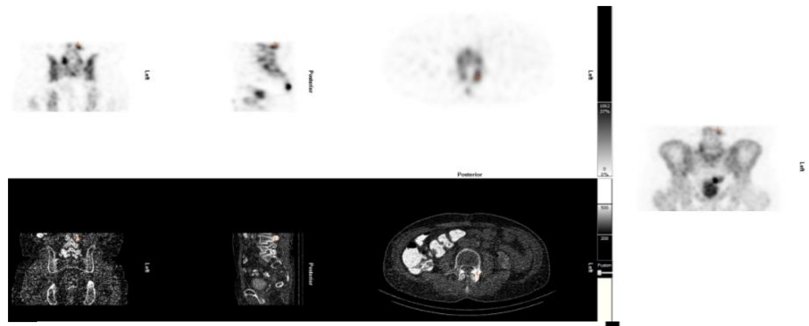

Staging III
Metastasis Os sacrum

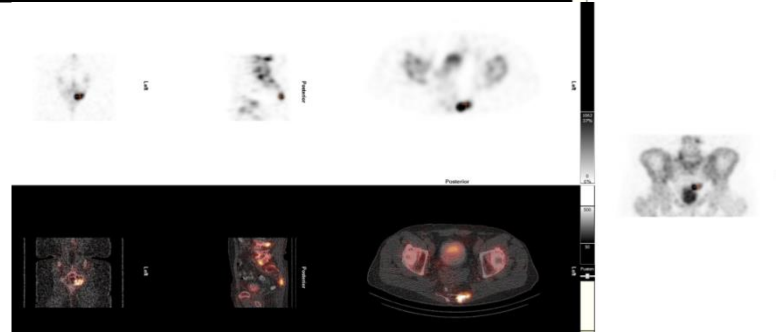

MIBG SPECT/CT

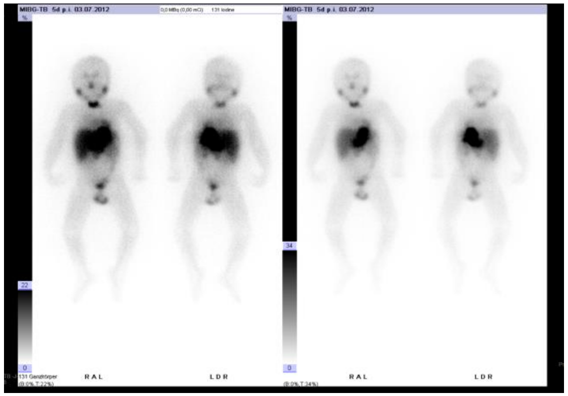

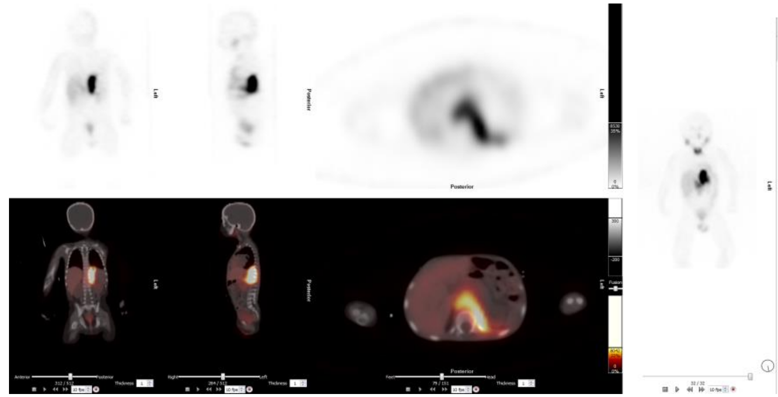

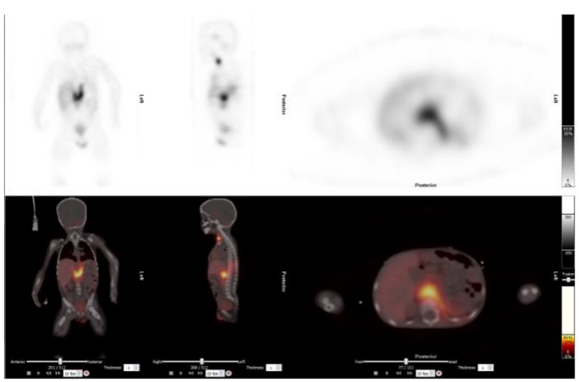

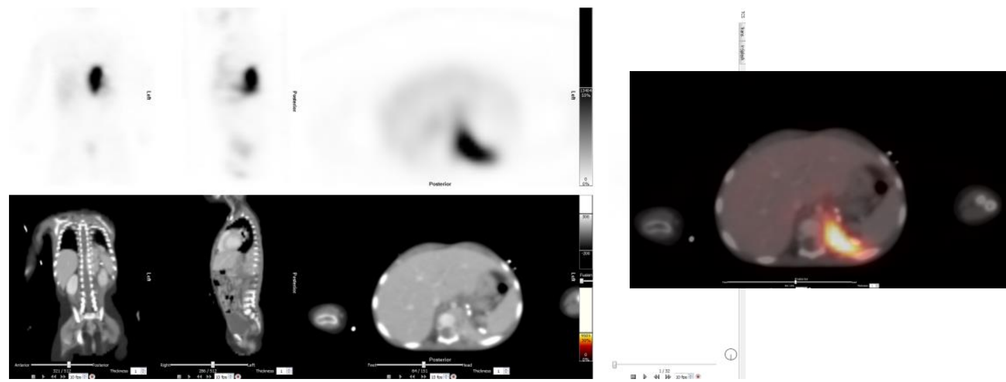

- 2 yrs., Neuroblastoma Stage IV, post therapy, Neuroplastoma recurrence with cerebral and abdominal metastases, Tumour progress under recurrence therapy
- Planar imaging and SPECT/CT with contrast agent 5 days post therapy

PET/CT

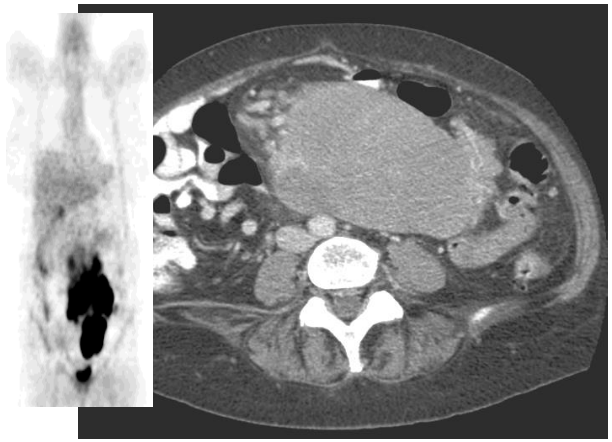

Patient 1

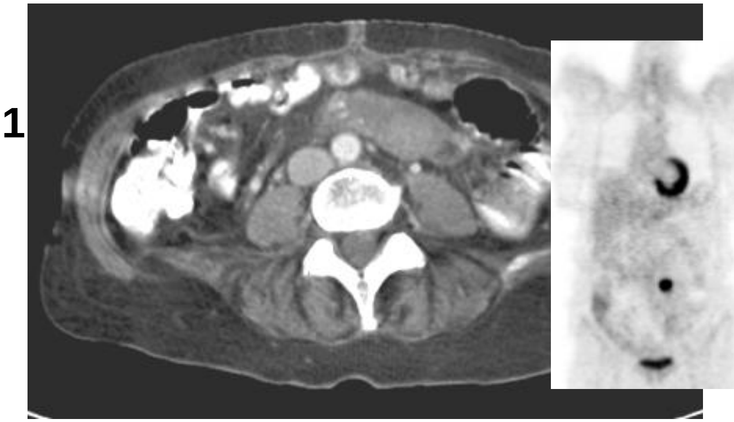

CRu (SPD – 84%)

Patient 2

PR (SPD – 55%)

PSMA PET/CT

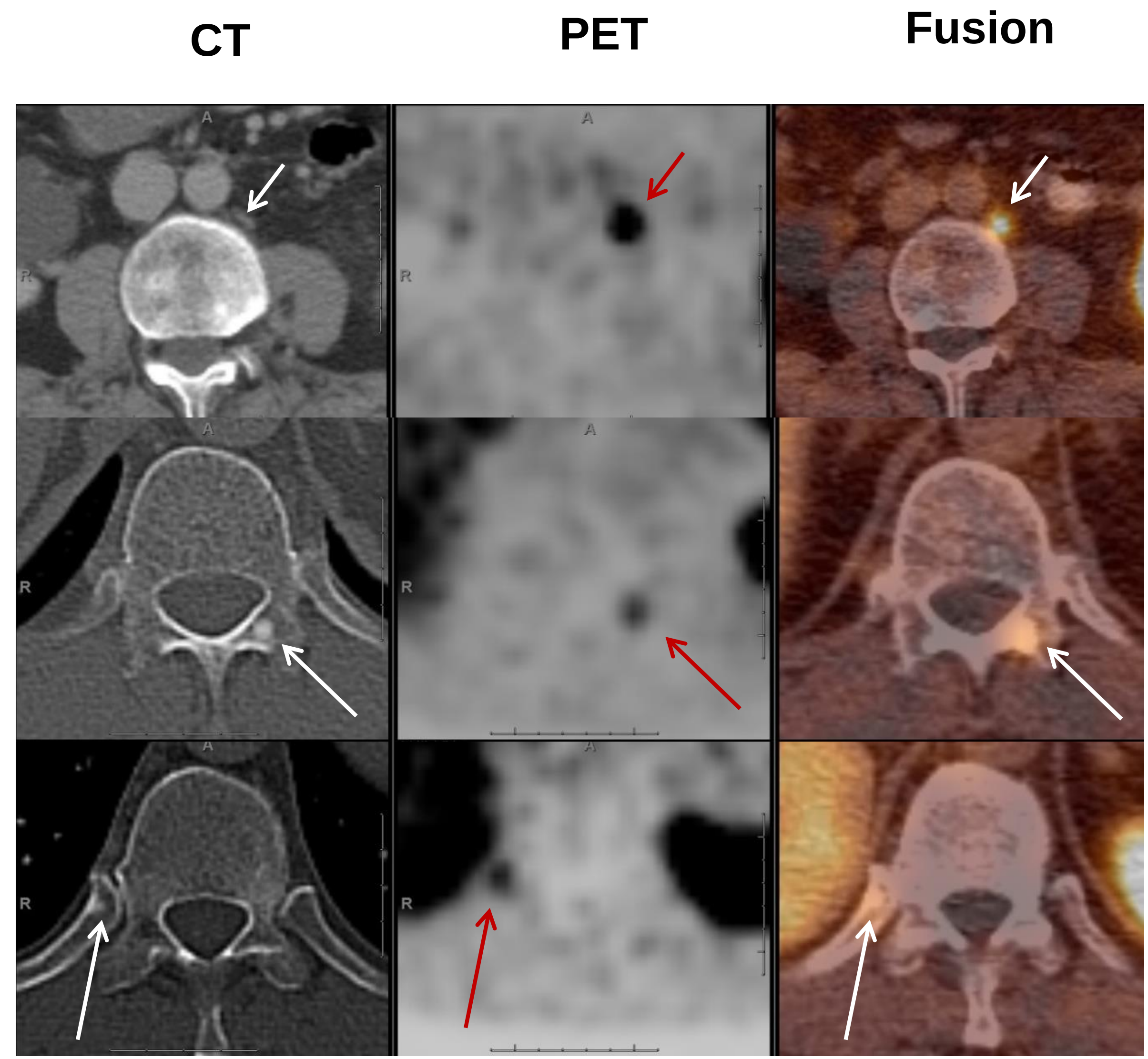

Bronchial carcinoid with sudden onset of blurry vision

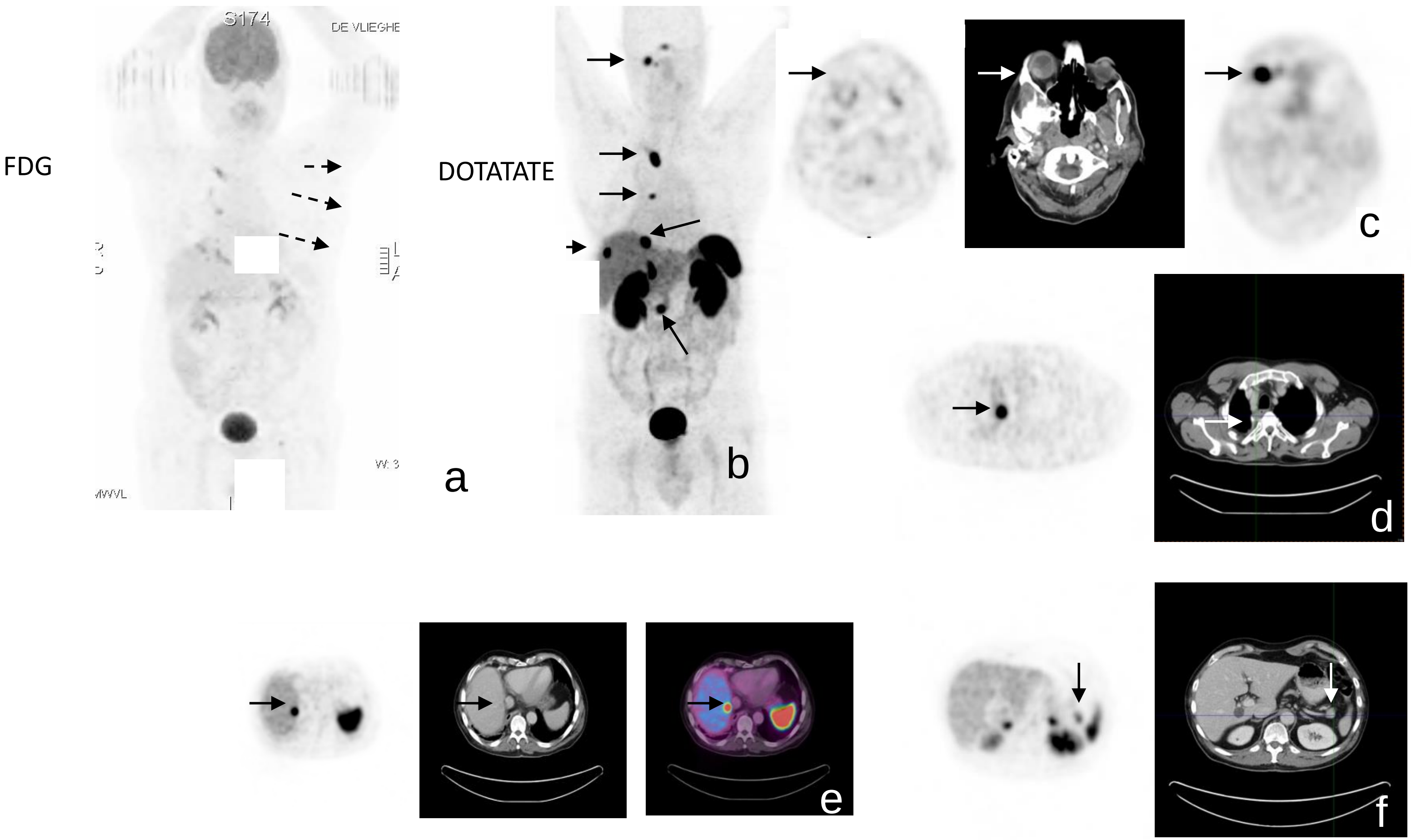

Small animal imaging

- Important for development of new tracer
- Final preclinical step in the process from bench to bedside

- µSPECT / CT
- µPET / CT

Small Animal Imaging / Model Examples

Small Animal -PET/CT

Small Animal – SPECT/CT


Small Animal – PET/SPECT/CT

Micro PET: Dedicated Small Animal System

- Micro PET Siemens Inveon

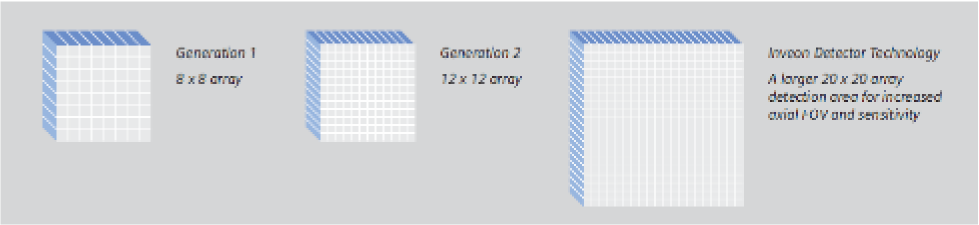

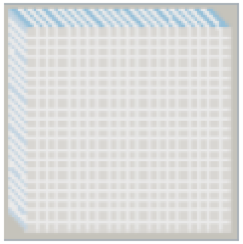

20x20 array

16 module

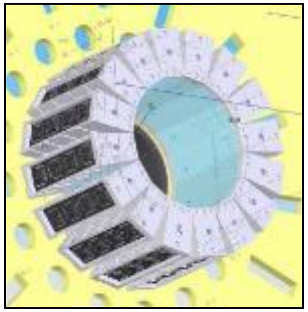

Detector diameter:	16,1 cm
Transaxial FOV:	10,0 cm
Axial FOV:	12,7 cm
Crystal-detectors:	LSO - 64 Blocks
	25600 Sum of single crystals
High resolution:	1,4 mm FWHM
Absolut Sensitivity:	100,0 cps / 1kBq , 10 %

Micro PET: Dedicated Small Animal System

Micro PET Siemens Inveon

Micro PET - measurement of the glucose metabolism with ^{18}F-FDG and of the skeleton with the bone affine radiopharmaceutical ^{18}F-NaF in a mouse.

^{18}F-Sodium fluoride

^{18}F-Fluorodesoxyglucose

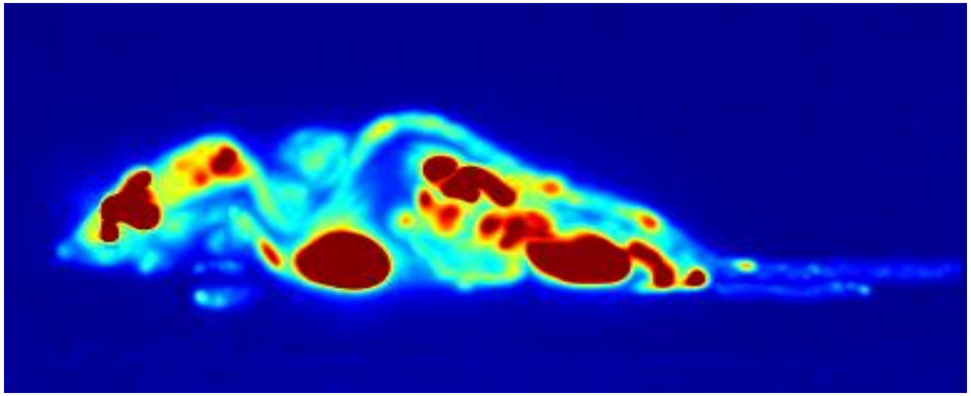

Digital PET Sub-System

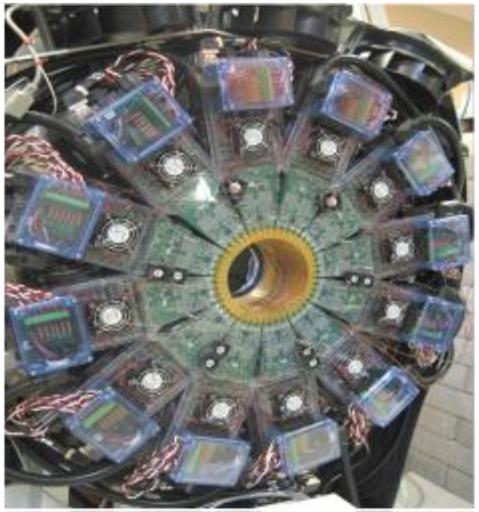

- Digital PET = direct coupling of scintillator to solid-state detectors
- No light sharing between detectors (better image quality)
- Patented Fast 3D Tomographic Image Reconstruction (December 2013)
- => Improved detectability of small lesions
- = > High count rate capability from very low activity to 80MBq
- => Superior image quality with excellent contrast ratio

◆ Bore diameter: 15cm

◆ Transaxial FOV: User-selectable 46-100 mm

◆ Axial FOV: 30cm (continuous motion)
  - LabPET4
  - LabPET8
  - LabPET12

- Quad-APD detector modules coupled with LYSO/LGSO phaswich scintillators
- Individual readout, parallel signal processing
- Fully integrated with SPECT and CT;
- field- upgradable

TriFoil

PET/CT Cardiac Imaging - Mouse

PET/CT:
0.7mCi of FDG, 20min. Post injection, 5 min. scan

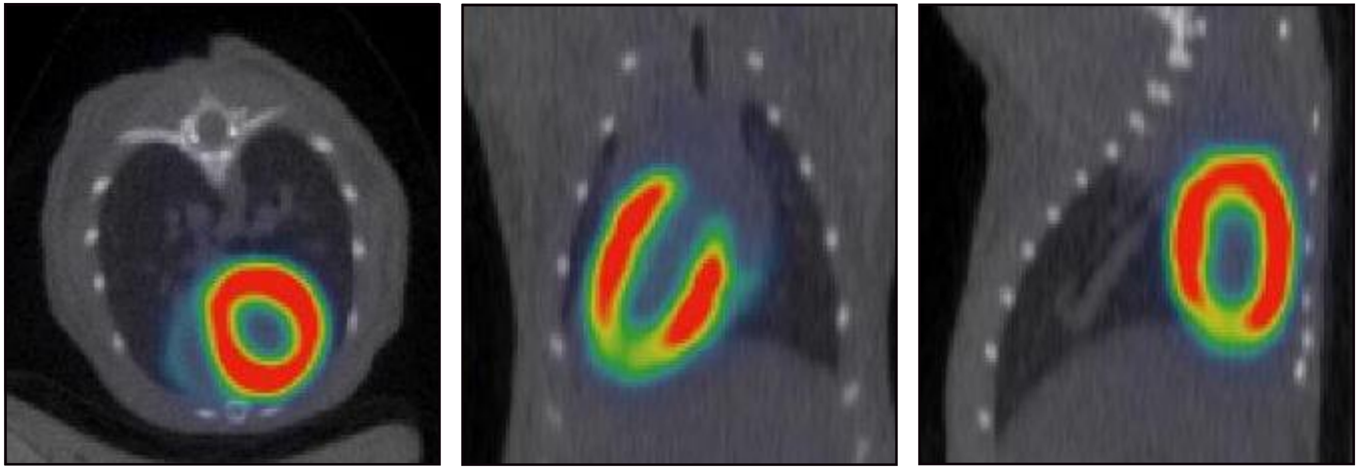

Detail of gated cardiac images

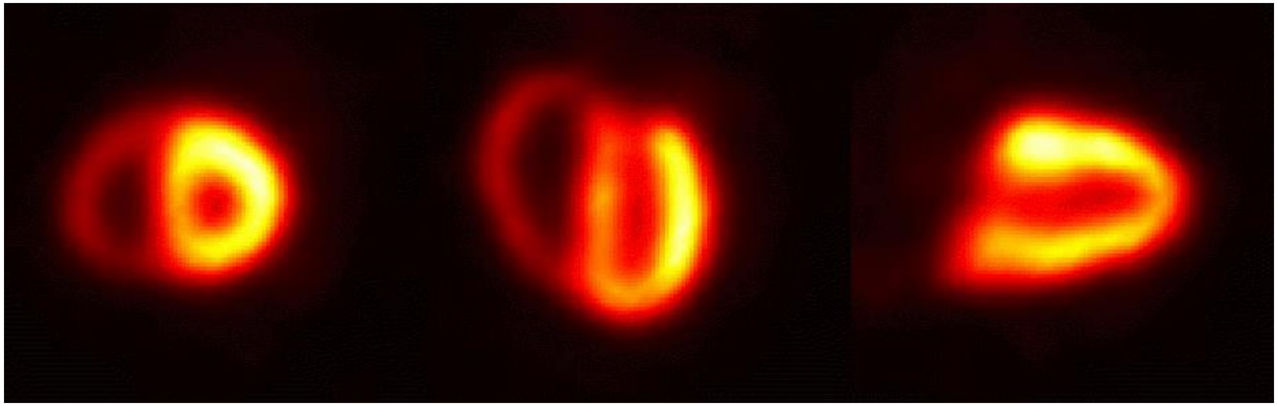

Courtesy of Dr. Ren-Shyan Liu, National Yangming University, Taipei, Taiwan

Excellent isotropical resolution: 185 g rat

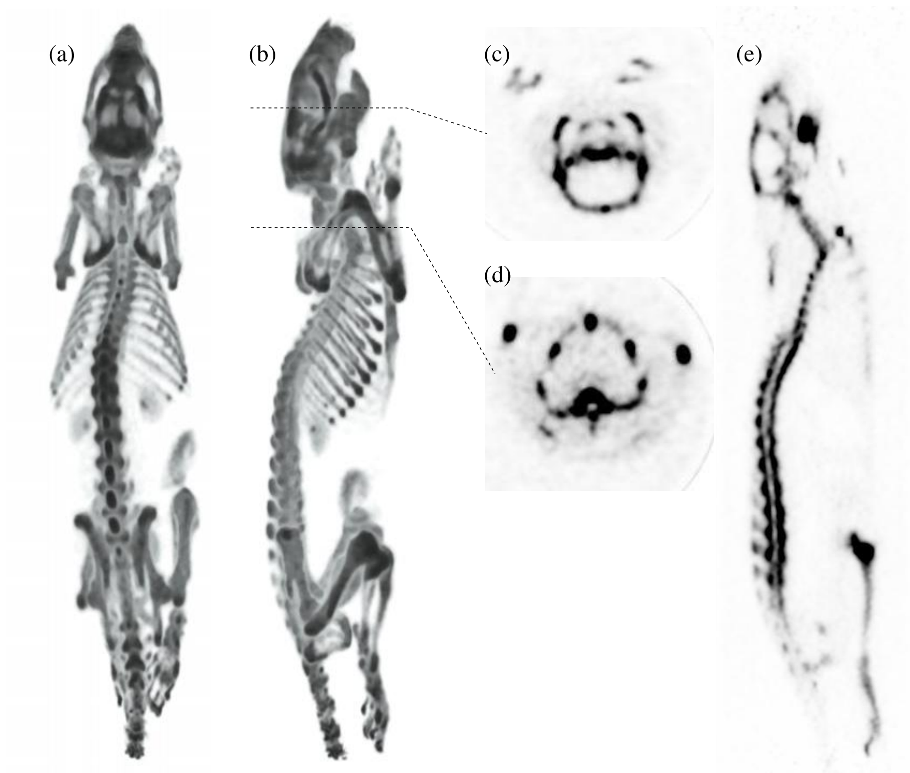

LabPET 8

Figure 10. Volume-rendered images (a), (b) of a 185 g rat injected with 31 MBq of $Na^{18}F$ and scanned 68 min post-injection on the LabPET8. Transaxial slices of the skull (c) and the ribcage (d) and a sagittal slice (e) are shown. The whole-body image was obtained by acquiring five overlapping decay-compensated scans with 3.78 cm steps for a total of 60 min. The image was obtained with a lower energy threshold of 350 keV and reconstructed using 80 3D MLEM iterations.

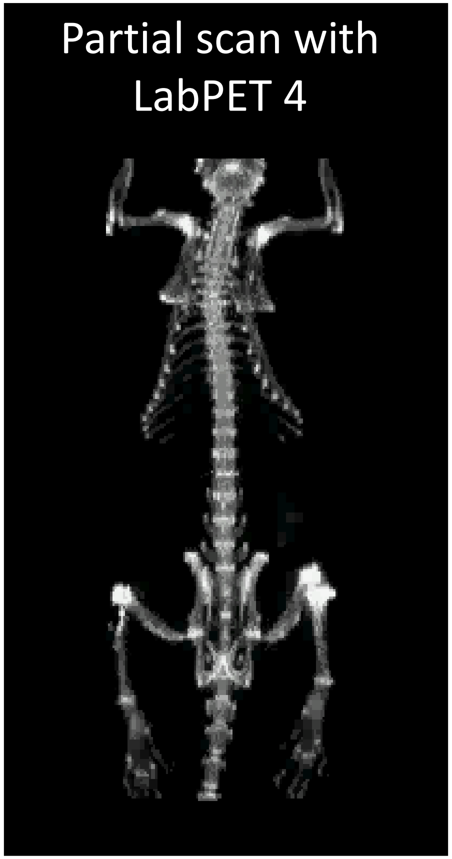

Reference: Imaging performance of LabPET APD-based digital PET scanners for pre-clinical research; M. Bergeron et al.; Universite de Sherbrooke, QC, Canada; Phys. Med. Biol. 59 (2014) 1–18

TriFoil

Small Animal Imaging / Model Examples

Small Animal -SPECT/CT

Small Animal -SPECT/CT

MMP - S P E C T

Micro SPECT: Measurement of the bone skeleton with ^{99m}Tc-HDP

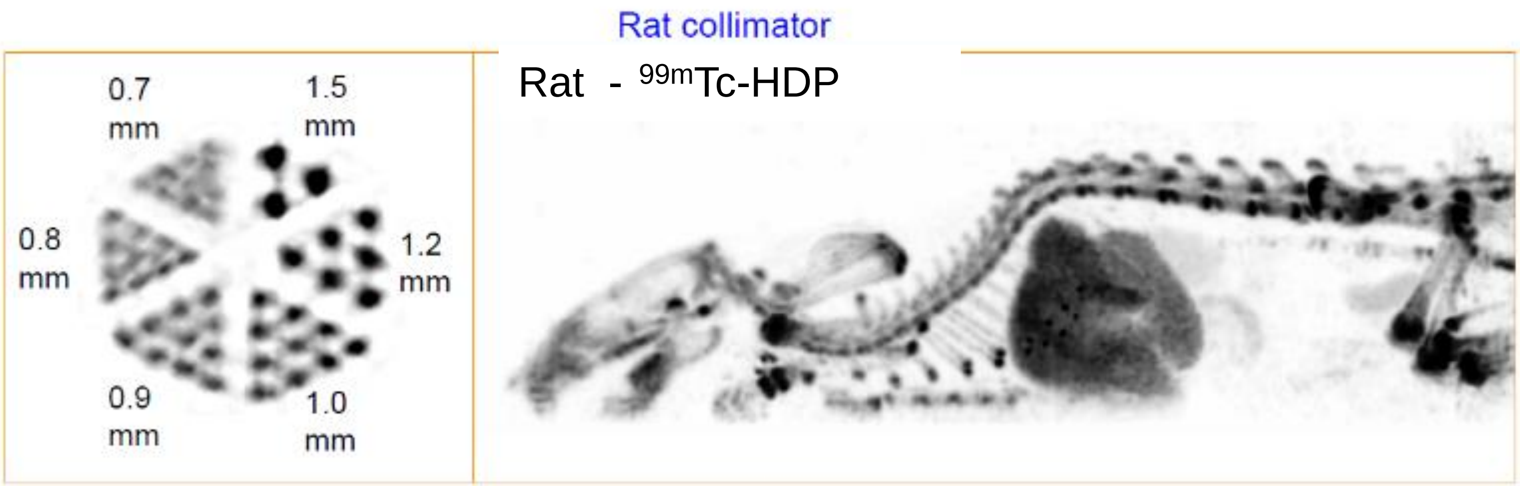

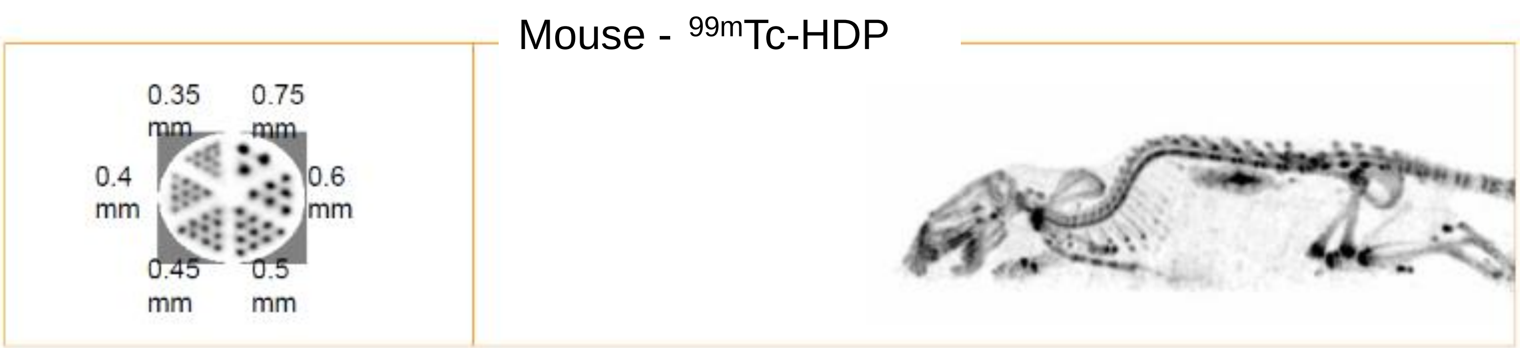

U-SPECT-II

^{99m}Tc-MIBI

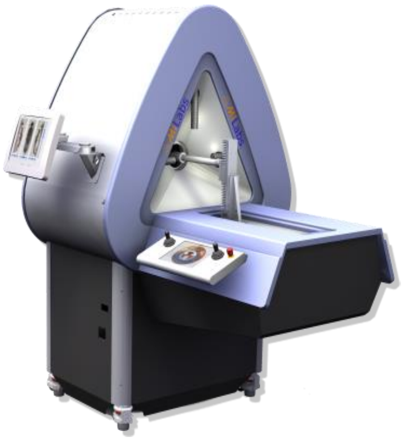

ECG gating

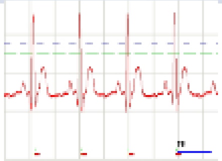

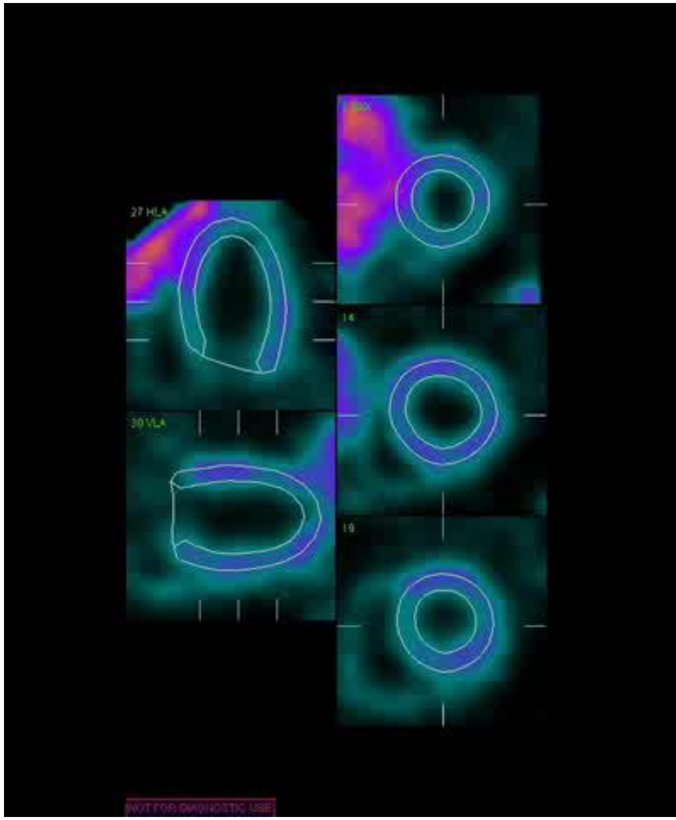

CARDIAC PMOD – 17 segment model

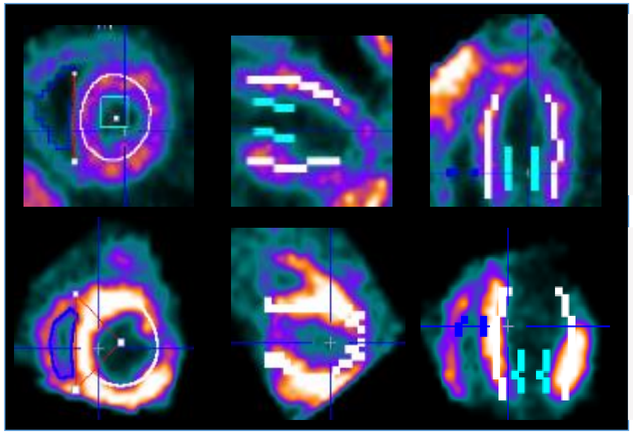

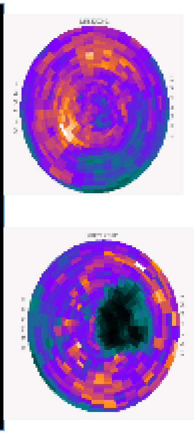

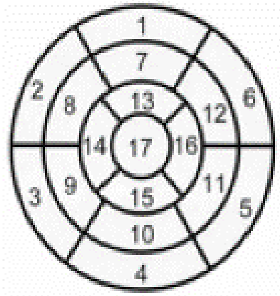

1. basal anterior
2. basal anteroseptal
3. basal inferoseptal
4. basal inferior
5. basal inferolateral
6. basal anterolateral
7. mid-anterior
8. mid-anteroseptal
9. mid-inferoseptal
10. mid-inferior
11. mid-inferolateral
12. mid-anterolateral
13. apical anterior
14. apical septal
15. apical inferior
16. lateral
17. apex

Multiplex Multi Pinhole (MMP) - S P E C T

- Micro SPECT: MMP-Technology with a clinically used SPECT gamma camera
  - Physical measuring principals
  - Characterisation and performance parameters

Siemens SPECT E.cam gamma camera

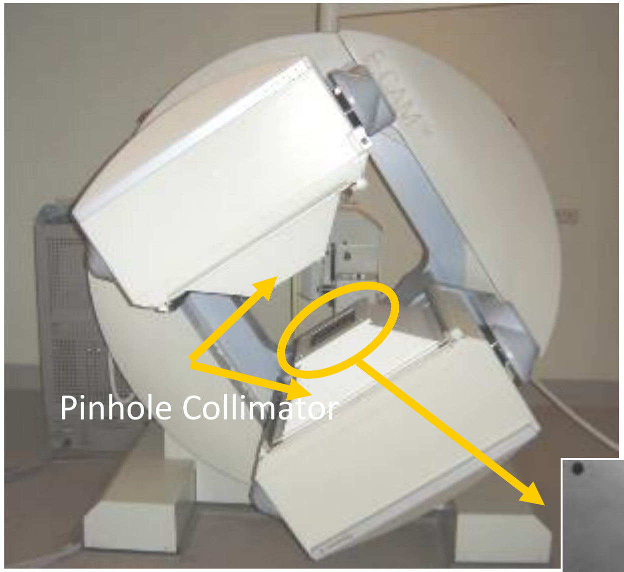

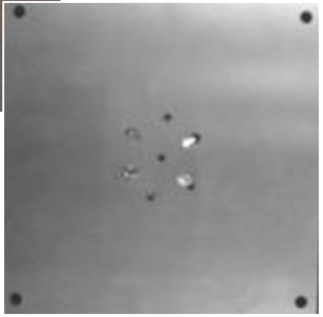

7-Pinhole Aperture Plate

MMP - S P E C T

MMP - S P E C T

Micro SPECT: Measurement with MMP-Technology by a clinically used SPECT gamma camera

SPECT

^{99m}Tc-HDP

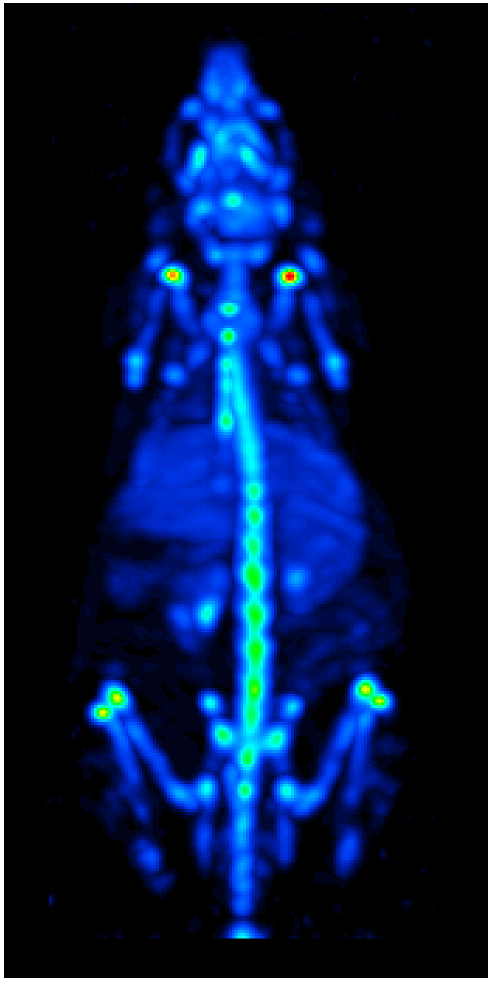

MMP - S P E C T

Micro SPECT: Measurement of a mouse bone skeleton with **^{99m}Tc-HDP**

CT

^{99m}Tc-Hydroxy-Diphosphonat

Fusion

CT - ^{99m}Tc-HDP SPECT

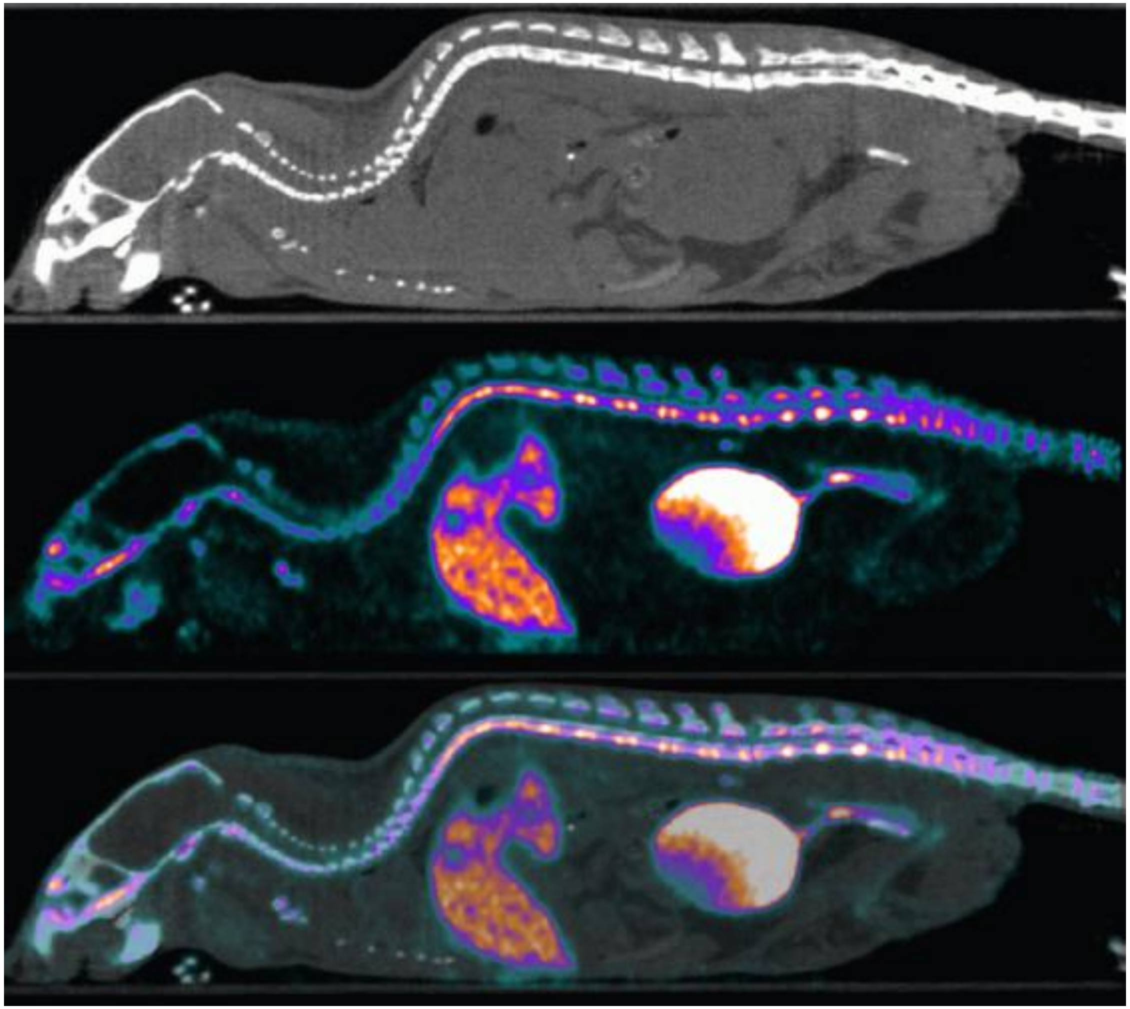

Biodistribution of ^{123}I-5-iodo-4´-thio-2´-deoxyuridine (^{123}I-ITdU) in WiDr xenografted mouse models - MMP µSPECT, 10.0 MBq 60 min p.i.

CT

µSPECT [^{123}I]-ITdU

FdUrd-Appl.

Fusion

µSPECT [^{123}I]-ITdU + CT

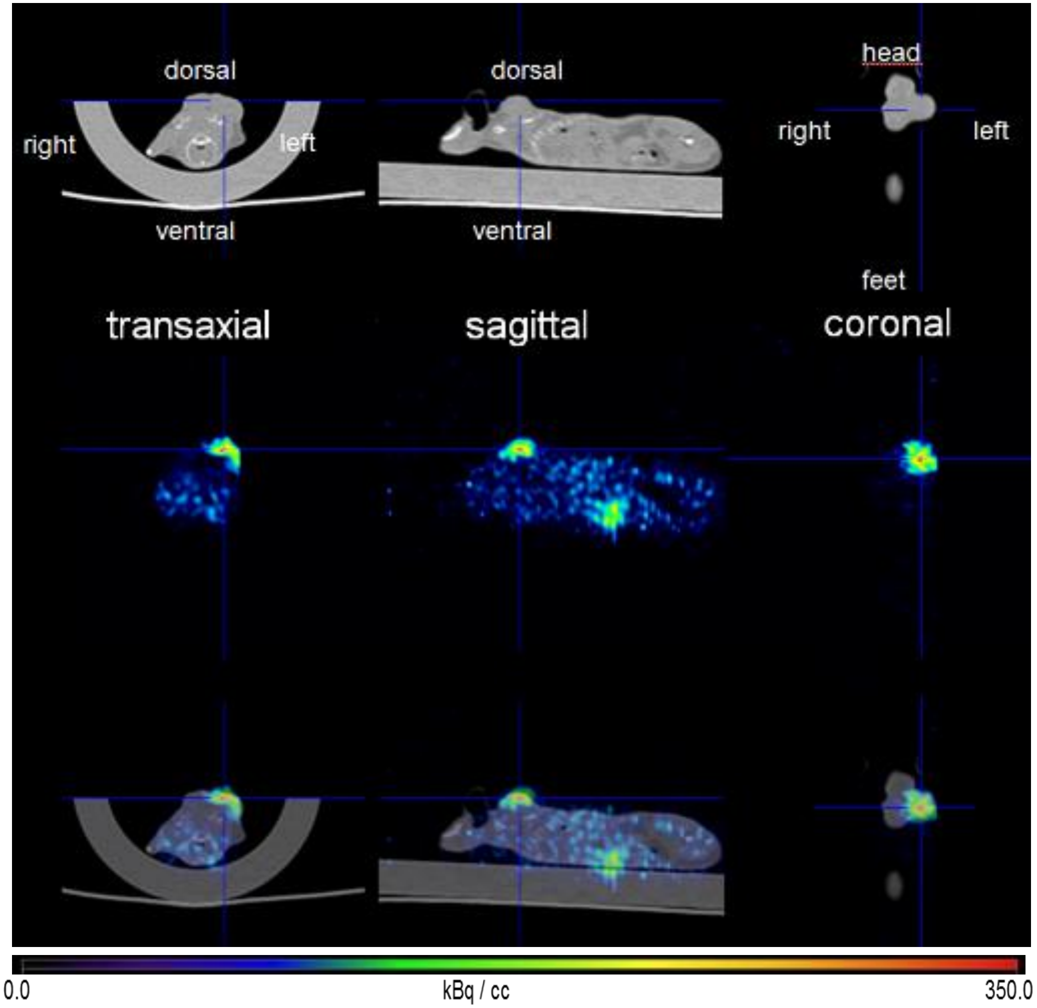

Examples for small animal imaging: biodistribution studies play a major role

- **New tracer development**
- **New pharmaca development**
- **Therapy studies**

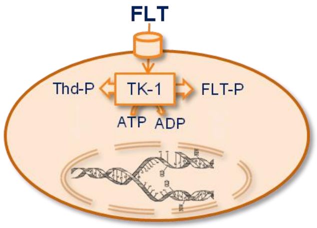

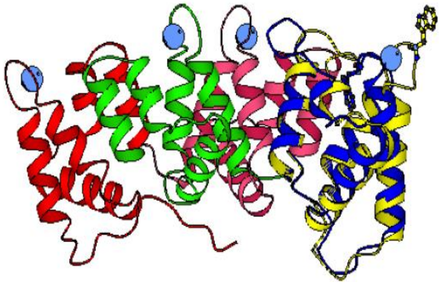
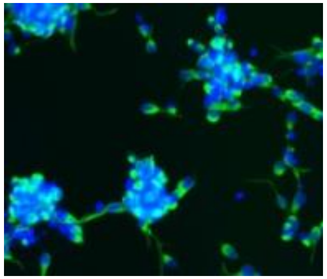
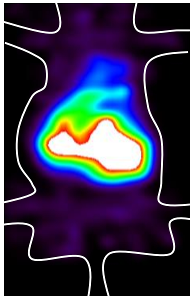
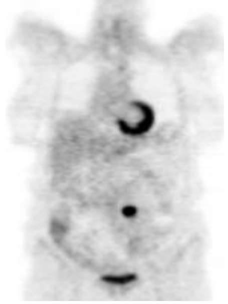

Indomethacin derivates targeting COX2

Indomethacin as chemical lead

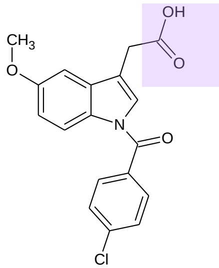

Derivatitation at carbonic acid ⇒ Indometacin-Derivate with different Polarity and charge for labeling with radio iod und radio fluor

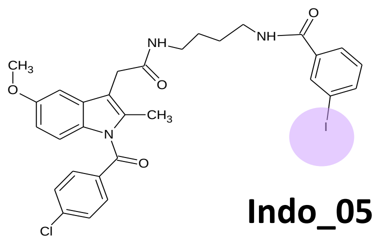

Indo_05

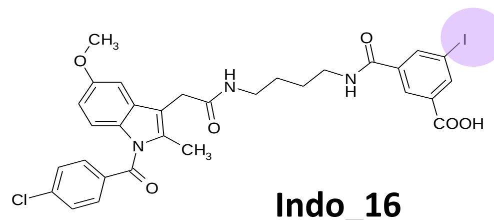

Indo_16

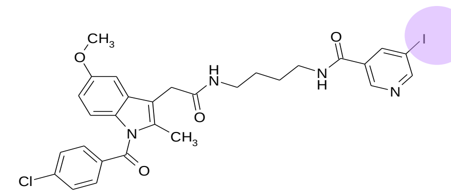

Indo_23

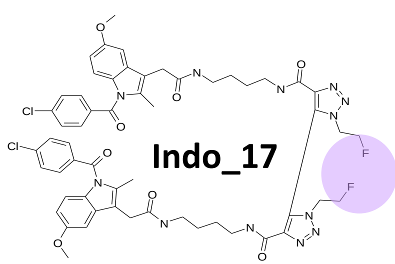

Indo_17

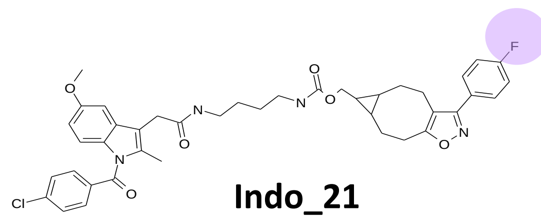

Indo_21

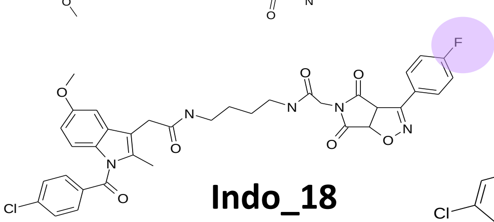

Indo_18

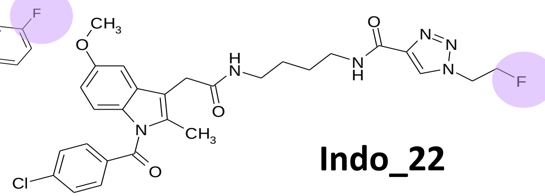

Indo_22

Cite this: *Chem. Commun.*, 2012, **48**, 7134–7136

www.rsc.org/chemcomm

COMMUNICATION

Beyond azide–alkyne click reaction: easy access to ^{18}F-labelled compounds *via* nitrile oxide cycloadditions†

Boris D. Zlatopolskiy,[ab] René Kandler,[b] Diana Kobus,[b] Felix M. Mottaghy[ac] and Bernd Neumaier[a,b]

Applied Radiation and Isotopes 70 (2012) 184–192

Contents lists available at SciVerse ScienceDirect

Applied Radiation and Isotopes

journal homepage: www.elsevier.com/locate/apradiso

ELSEVIER

C-(4-[^{18}F]fluorophenyl)-N-phenyl nitrone: A novel ^{18}F-labeled building block for metal free [3+2]cycloaddition

Boris D. Zlatopolskiy[a,b], René Kandler[a], Felix M. Mottaghy[b,c], Bernd Neumaier[a,*]

[a] Max Planck Institute for Neurological Research, Gleueler Straße 50, 50931 Cologne, Germany
[b] Klinik für Nuklearmedizin, Aachen University, RWTH, Pauwelsstr. 30, 52074 Aachen, Germany
[c] Department of Nuclear Medicine, Maastricht University Medical Center, P. Debyelaan 25, 6229HX Maastricht, the Netherlands

Biodistribution of nucleosid analogues

PET [18F]FLT	µSPECT [^{123}I]-ITdU	µSPECT [^{123}I]-ITdU
FdUrd-Appl.	FdUrd-Appl. 60 min p.i.	FdUrd-Appl. 24 h p.i.

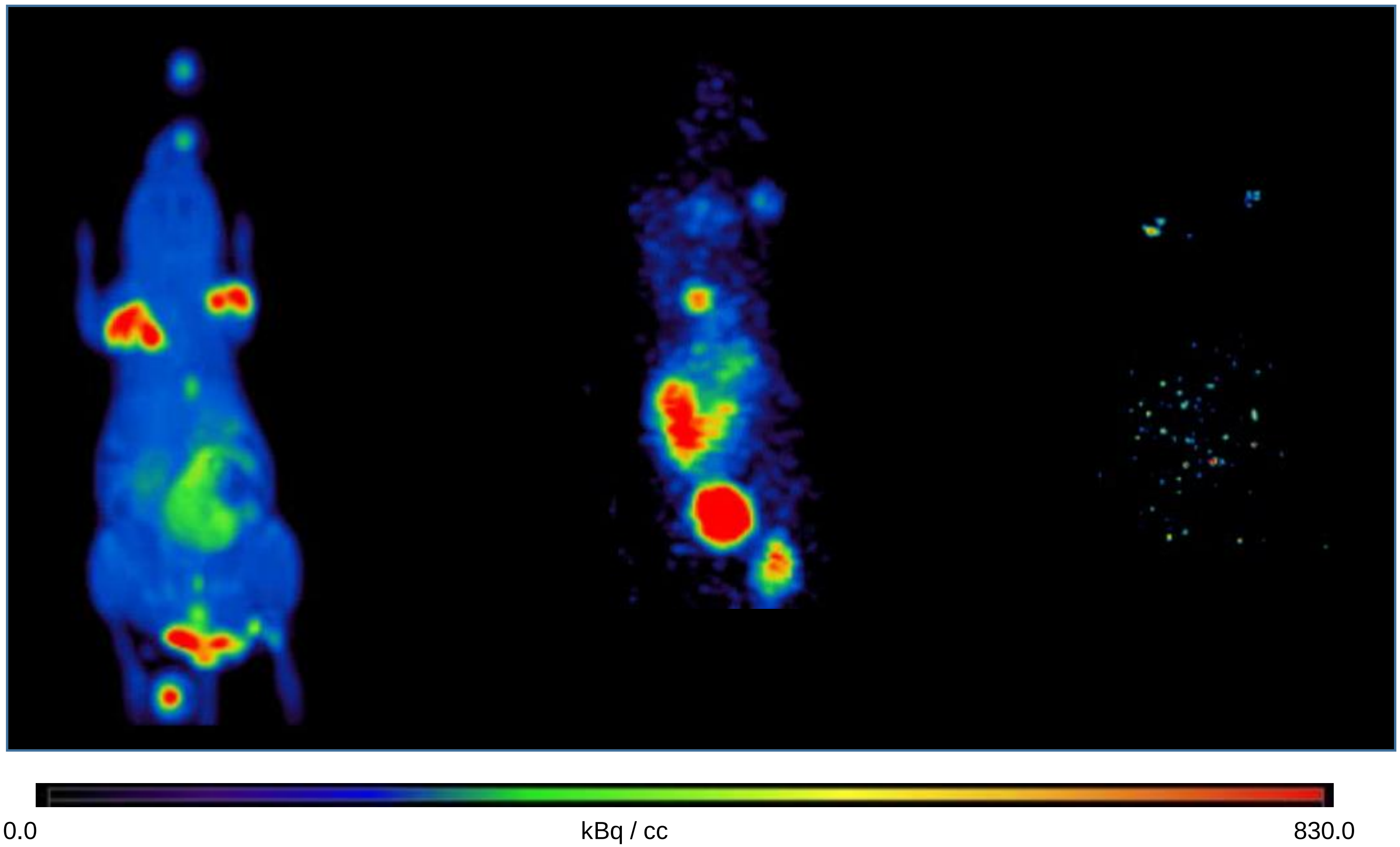

COX2-specific Inhibitors: PET-Tracer

Cellular uptake of COX2-PET Tracer: Competition study with cold standards and [I-125]Indo_23 as COX2 Tracer und corresponding PhosphorImager and Western Blot Analysis

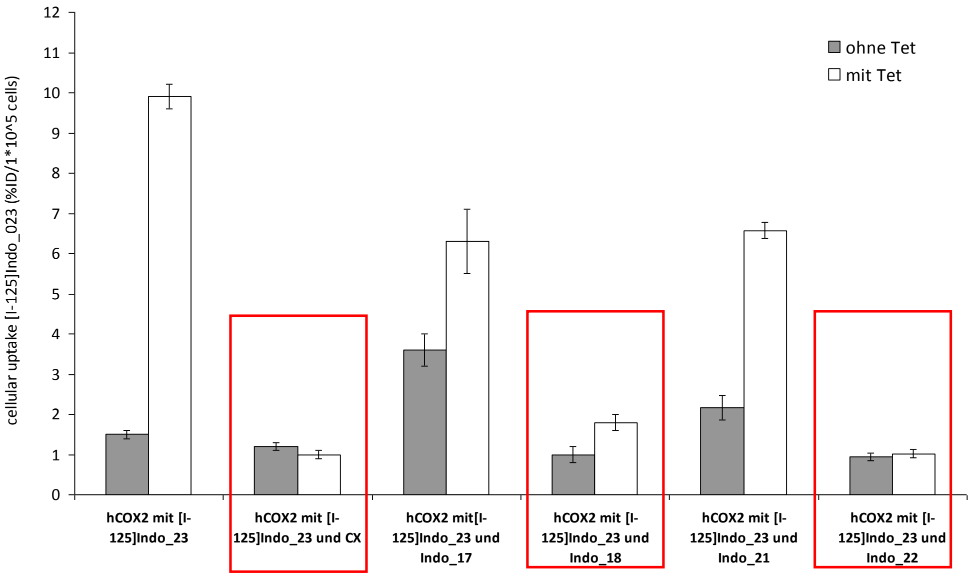

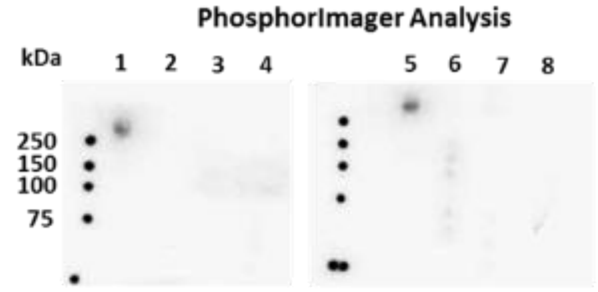

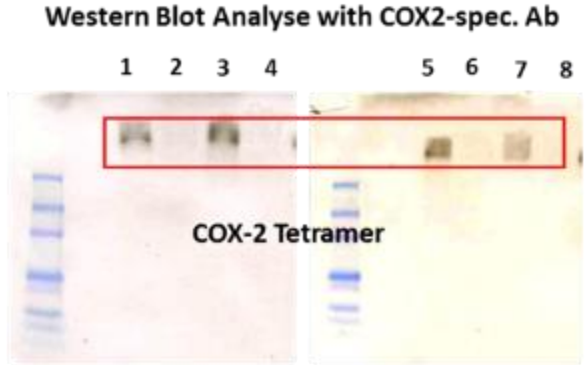

1. HEK COX-2 mit [I-125]Indo_23, Tet stimulated
2. HEK COX-2 [I-125]Indo_23, unstimulated
3. HEK COX-2 mit [I-125]Indo_23 + CX, Tet stimulated
4. HEK COX-2 mit [I-125]Indo_23 + CX, unstimulated
5. HEK COX-2 mit [I-125]Indo_23 + Indo_21, Tet stimulated
6. HEK COX-2 mit [I-125]Indo_23 + Indo_21unstimulated
7. HEK COX-2 mit [I-125]Indo_23 + Indo_22, Tet stimulated
8. HEK COX-2 mit [I-125]Indo_23 + Indo_22, unstimulated

Morgenroth, Zlatopolskiy, Mottaghy et al.

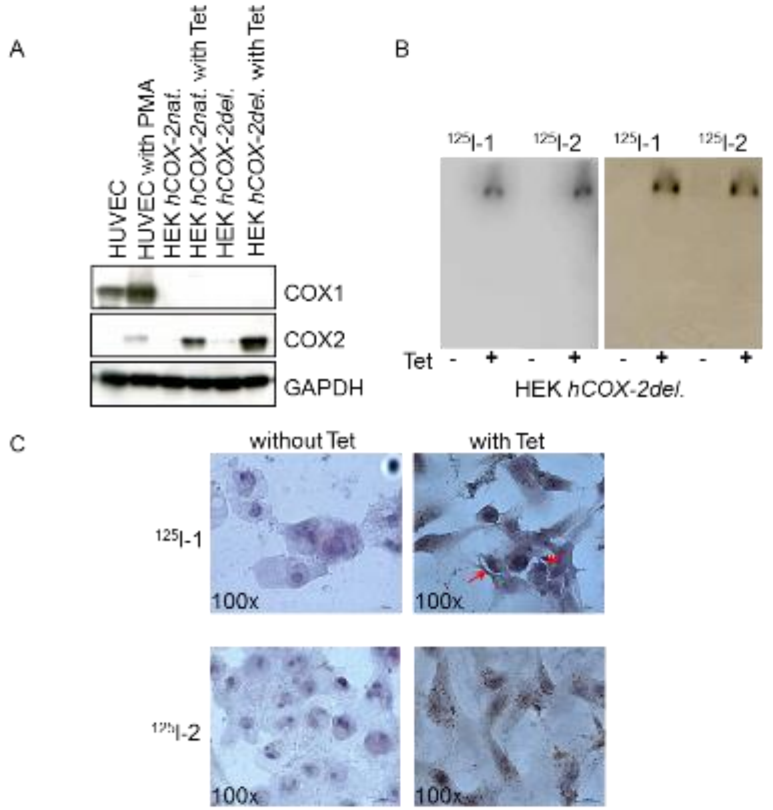

Fig. 3. Binding specificity and intracellular distribution of iodinated indomethacin derivatives. (A) SDS and western blot analysis od COX-1 and COX-2 expression in HUVEC, HEK hCOX-2*nat* and HEK hCOX-2*del* cells in dependency on PMA- and Tet-stimulation, respectively. GAPDH served as a loading control. (B) SDS gel electrophoresis of cell lysates obtained from HEK *hCOX-2del* cells incubated with ^{125}I-**1** and ^{125}I-**2** and visualized by phosphorimager (*left*); subsequent western blot analysis with COX-2 specific antibody. (C) Intracellular localization of ^{125}I-**1** and ^{125}I-**2** in HEK hCOX-2*del* cells detected by microautoradiography followed by a standard H&E staining.

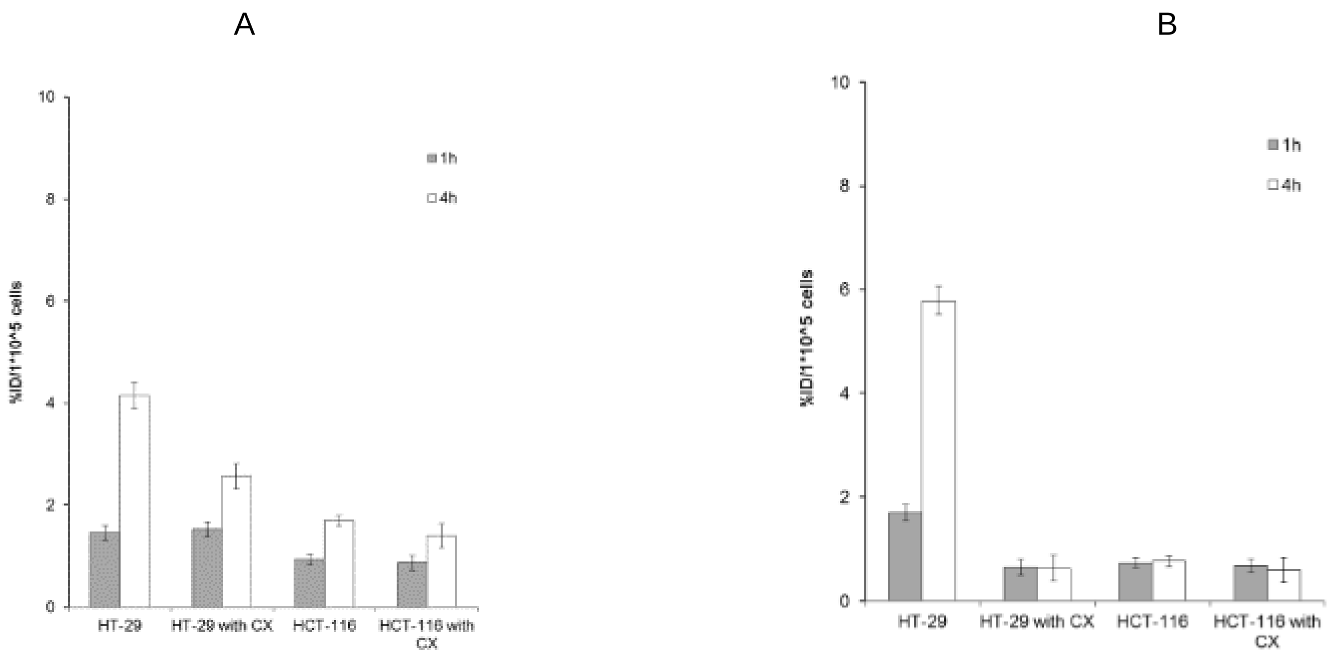

Fig. 4. Cellular uptake with ^{125}I-**1** and ^{125}I-**2** compounds in colon carcinoma cells after 1h and 4h incubation (in % of incubated dose (ID)/well). (A) Cellular uptake of ^{125}I-**1** in HT29 and HCT-116 cells w/o and with CX. (B) Cellular uptake of ^{125}I-**2** in HT29 and HCT-116 cells w/o and with CX.

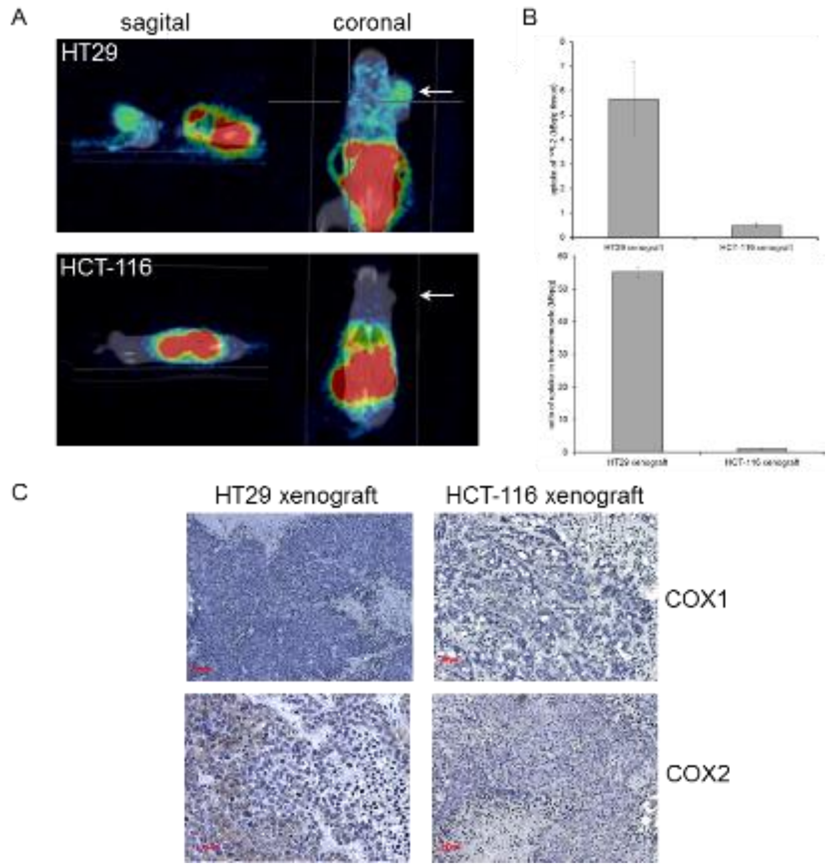

Fig. 5. *In vivo* study with ^{124}I-**2** compound in colon carcinoma xenografted SCID mice. (A) µPET/CT molecular imaging of COX-2 with^{124}I-**1** in HT29 (upper panel) and HCT-116 (lower pannel) xenografted SCID mice at 4h p.i.. (B) Uptake of ^{125}I-**2** in HT29 and HCT-116 tumors (in kBq/g tissue) (upper panel); tumor to muscle uptake ratio of ^{125}I-**2** in HT29 and HCT-116 tumor xenografted mice (lower panel). (C) immunhistological analysis of COX-1 and COX-2 in HT29 and HCT-116 xenografts.

New pharmaca development

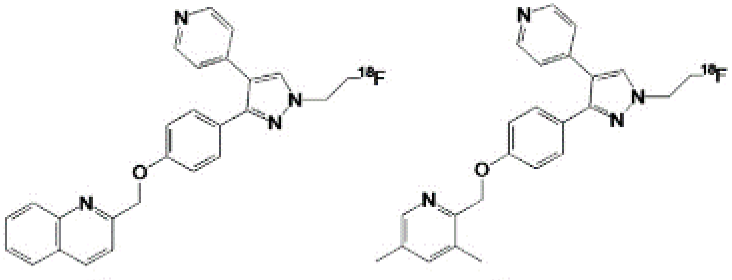

^{18}F-JNJ41510417 ^{18}F-JNJ42259152

Phosphodiesterase-10A (PDE10A) is implicated in several neuropsychiatric disorders involving basal ganglia neurotransmission, such as schizophrenia, obsessive–compulsive disorder and Huntington's disease.

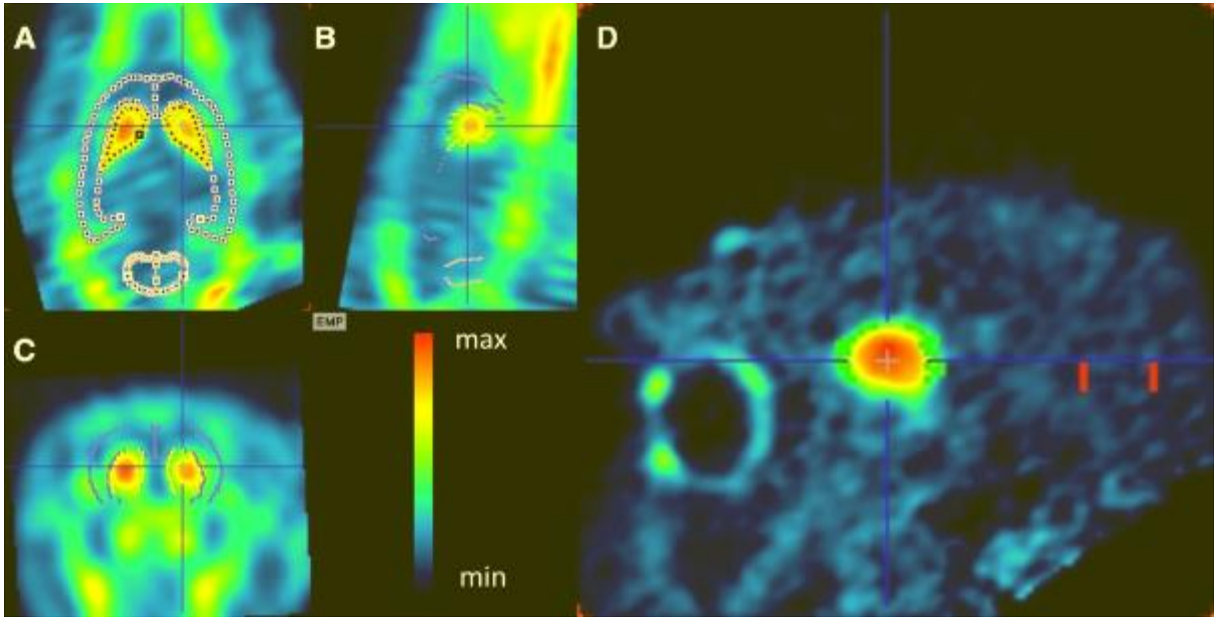

S. Celen et al. NeuroImage 82:13–22, 2013

New pharmaca development

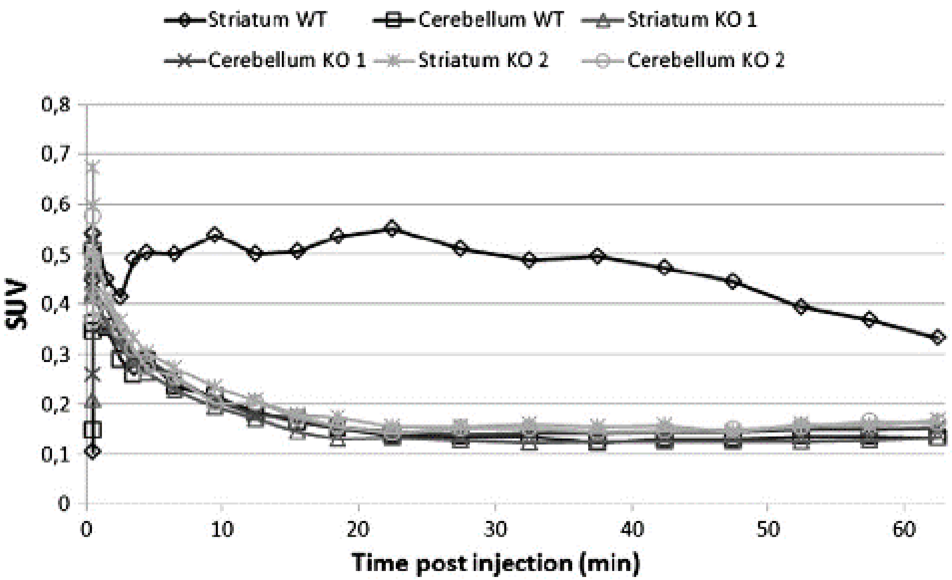

Small-animal PET transversal sections of KO (left image) and WT (right image) mouse brain injected with [18F]JNJ42259152 (summed images from 0 to 60 min post tracer injection). ROIs were drawn on the areas corresponding to striatum and cerebellum to obtain the TACs of [18F]JNJ42259152 in striatum and cerebellum of two PDE10A KO mice and one WT mouse (WT = wild type mouse, KO = PDE10A knock-out mouse).

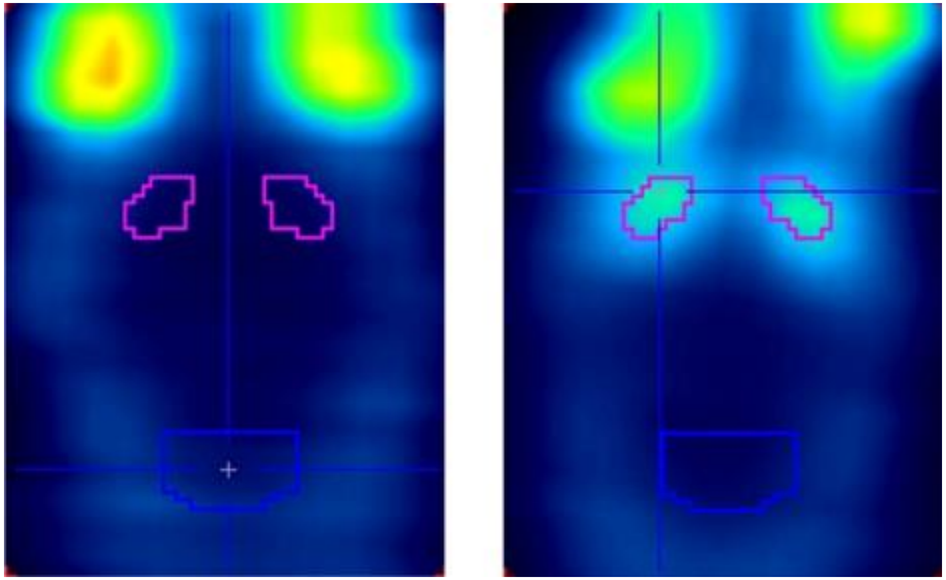

S. Celen et al. NeuroImage 82:13–22, 2013

Glucose metabolism: therapy response

^{18}F-FDG – PET

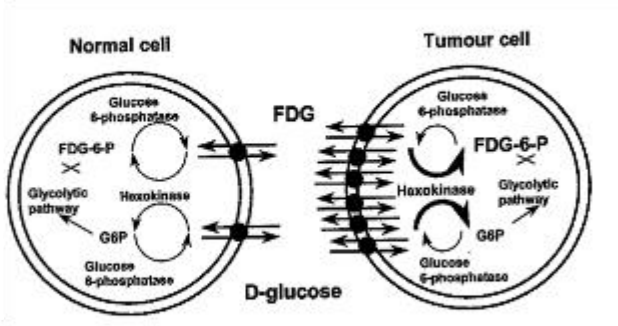

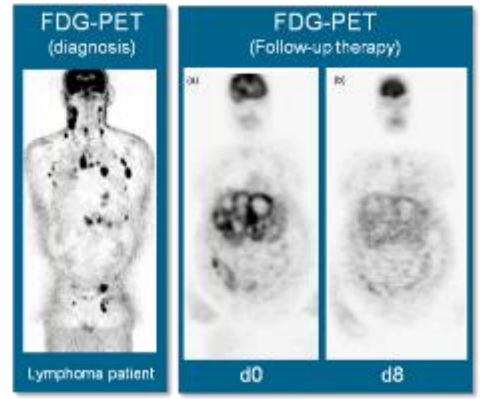

Stroobants et al., E J Cancer 2003

Eur J Nucl Med Mol Imaging (2010) 37:1688–1695
DOI 10.1007/s00259-010-1479-0

ORIGINAL ARTICLE

Dose-response relationship in cyclophosphamide-treated B-cell lymphoma xenografts monitored with [^{18}F]FDG PET

Lieselot Brepoels · Marijke De Saint-Hubert · Sigrid Stroobants · Gregor Verhoef · Jan Balzarini · Luc Mortelmans · Felix M. Mottaghy

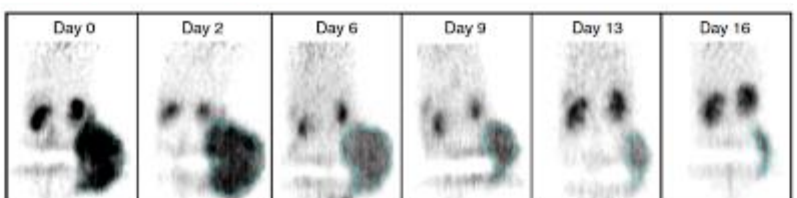

	Day 0	Day 2	Day 6	Day 9	Day 13	Day 16
Vol_{met} (ml)	3.3	3.2	2.8	1.6	0.4	0.3
$SUV_{mean}/liver_{mean}$	8	5	2.9	4.4	2.1	3.3
$SUV_{max}/liver_{mean}$	17.9	9.6	10.3	8.6	3.7	7.7
$TLG/liver_{mean}$	26.5	16	8	7.2	0.9	1

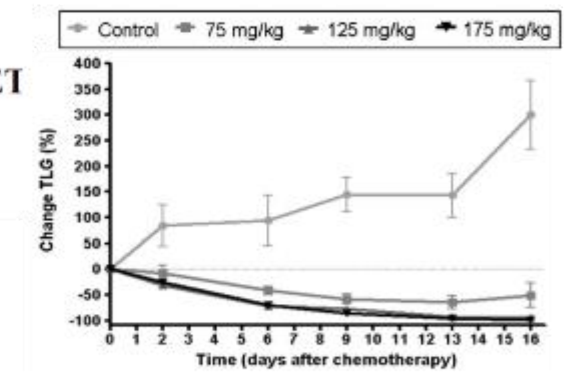

→ [18F]FDG –Uptake represents dose-effect-dependency of Cyclophosphamid

Proliferation: Therapy Response

^{18}F-FLT – PET

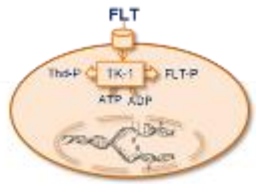

Am J Nucl Med Mol Imaging 2012;2(1):110-121
www.ajnmmi.us /ISSN:2160-8407/ajnmmi1111001

Original Article

Molecular imaging of therapy response with ^{18}F-FLT and ^{18}F-FDG following cyclophosphamide and mTOR inhibition

Marijke De Saint-Hubert[1], Lieselot Brepoels[2], Ellen Devos[3], Peter Vermaelen[2], Tjibe De Groot[3], Thomas Tousseyn[4], Luc Mortelmans[2], Felix M Mottaghy[1,2,5]

[1]Department of Nuclear Medicine, Maastricht University Medical Centre, Maastricht, The Netherlands; [2]Department of Nuclear Medicine, Katholieke Universiteit Leuven, Leuven, Belgium; [3]Laboratory for Radiopharmacy, Katholieke Universiteit Leuven, Leuven, Belgium; [4]Morphology and Molecular Pathology, Katholieke Universiteit Leuven, Leuven, Belgium; [5]Department of Nuclear Medicine, University Hospital RWTH Aachen, Germany

Received November 5, 2011; accepted November 18, 2011; Epub December 15, 2011; Published January 1, 2012

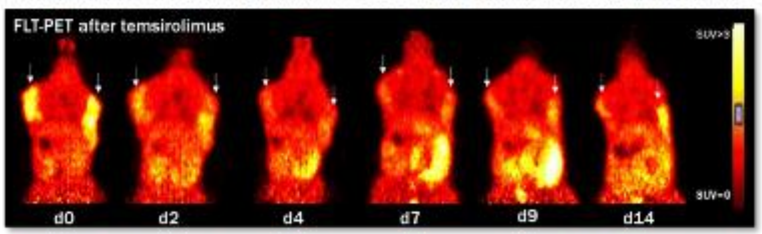

→ FLT-PET represents reduced proliferation after temsirolismus.

→Correlates with the end of mitosis (Increase of G0/G1 in Facs) and ki67- staining

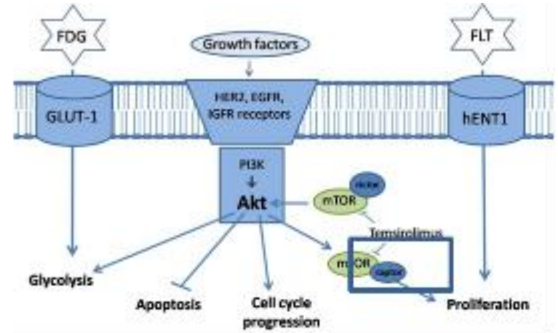

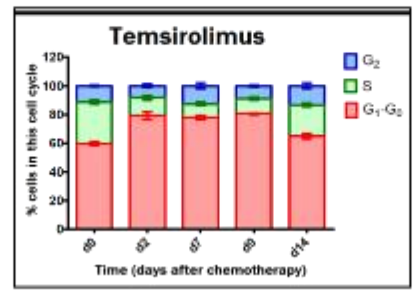

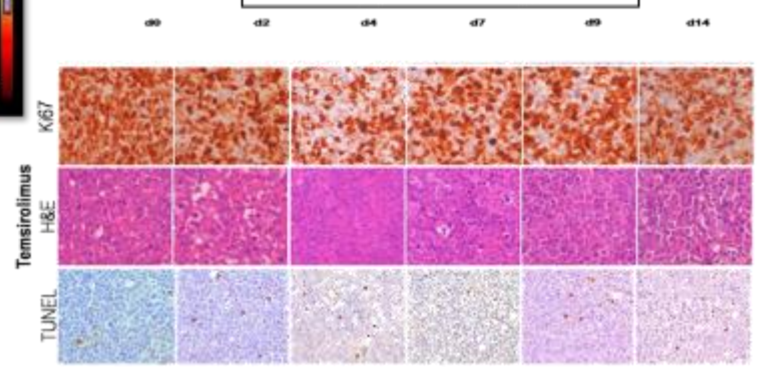

Take home

- SPECT and PET
  - provide a broad spectrum of diagnostic approaches
  - help to understand biological processes
  - are an important link in the „bench to bedside“ concept of probe development
- Molecular Imaging
  - is important for non-invasive monitoring of disease
  - supports development of new theranostic concepts